POWDER ROCKET FEASIBILITY EVALUATION

H. Joseph Loftus, et al

Bell Aerosystems Company

Prepared for:

Air Force Rocket Propulsion Laboratory

April 1973

UNCLASSIFIED

Security Classification

AD 769283

DOCUMENT CONTROL DATA - R & D

(Security classification of title, body of abstract and indexing annotation must be entered when the overall report is classified)

1. ORIGINATING ACTIVITY (Corporate author) Bell Aerospace Company Post Office Box One Buffalo, New York 14240	2a. REPORT SECURITY CLASSIFICATION Unclassified 2b. GROUP

3. REPORT TITLE

POWDER ROCKET FEASIBILITY EVALUATION

4. DESCRIPTIVE NOTES (Type of report and inclusive dates)

FINAL TECHNICAL REPORT

5. AUTHOR(S) (First name, middle initial, last name)

R. J. Loftus, D. Marshall, L. N. Montanino

6. REPORT DATE	7a. TOTAL NO. OF PAGES	7b. NO. OF REFS
APRIL 1973	~~74~~ 98	11

8a. CONTRACT OR GRANT NO	9a. ORIGINATOR'S REPORT NUMBER(S)
F04611-72-C-0045 b. PROJECT NO 3058	8651-928001 9b. OTHER REPORT NO(S) (Any other numbers that may be assigned this report)

10. DISTRIBUTION STATEMENT

Approved for public release; distribution unlimited.

11. SUPPLEMENTARY NOTES	12. SPONSORING MILITARY ACTIVITY
	Air Force Rocket Propulsion Laboratory Edwards Air Force Base California 93523

13. ABSTRACT

The objective of this evaluation was to investigate the feasibility of the powder rocket concept.

A series of rocket combustor tests were conducted at 500 and 900 pound thrust levels, utilizing ammonium perchlorate/aluminum propellants. Eight 500 pound thrust fire tests were conducted to determine the effect of propellant variations on combustion. Particle size affected combustion stability with smoother combustion obtained with reduced particle size. Combustion oscillations of ±5 percent of mean chamber pressure at a frequency of 140 Hertz occurred utilizing 3 micron (X-65) Al and 20 micron AP which was the smoothest fire test. However, partial plugging of the AP injector occurred which was attributed to the agglomeration tendency of the finer AP. A test with AP containing 0.2 weight percent silica additive, improved the AP flow character but increased combustion oscillation level to ±38 percent of mean Pc.

Six 900 pound thrust fire tests were conducted with scaled-up hardware utilizing a 50/50 by weight blend of 55 and 20 micron AP, with 3 micron (X-65) Al. Combustion oscillation amplitude ranged from ±18 to ±7 percent of mean chamber pressure.

Maximum specific impulse performance efficiency derived was 0.90 with the 900 pound thrust hardware and 0.93 for the 500 pound units.

A laboratory powder packing investigation was conducted to establish methods to maximize density of the AP powder. Some packing tests were performed with AP/Al mixtures. Results showed maximum packed density/particle density ratio of 0.77 for AP, and 0.75 for AP/Al mixtures.

DD FORM 1 NOV 68 1473

(Continued next page)

UNCLASSIFIED

Security Classification

14. KEY WORDS	LINK A		LINK B		LINK C	
	ROLE	WT	ROLE	WT	ROLE	WT
Powder Propellants						
Rocket Engine						
Combustion						
Fluidization						
Particle Packing						

NOTICES

When U.S. Government drawings, specifications, or other data are used for any purpose other than a definitely related Government Procurement operation, the Government thereby incurs no responsibility nor any obligation whatsoever, and the fact that the Government may have formulated, furnished, or in any way supplied the said drawings, specifications, or other data is not to be regarded by implication or otherwise, as in any manner licensing the holder or any other person or corporation, or conveying any rights or permission to manufacture, use or sell any patented invention that may in any way be related thereto.

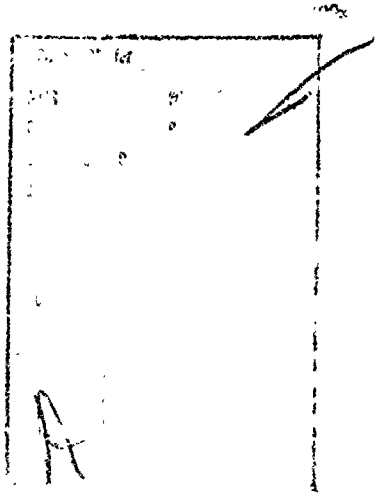

AFRPL-TR-73-22

POWDER ROCKET

EVALUATION PROGRAM

H. J. Loftus, D. Marshall, L. N. Montanino

FOREWORD

This report covers the work performed by Bell Aerospace during the period 21 February 1972 through 1 March 1973 on the Powder Rocket Evaluation Program, for the Air Force Rocket Propulsion Laboratory, Technology Division, Edwards Air Force Base, California. The effort was performed in accordance with Contract FO4611-72-C-0045, under the direction of Air Force Project Engineer, Dr. D. George, RTSC.

The Bell Aerospace Project Manager/Technical Director was Mr. H. Joseph Loftus. Other principal contributors in accomplishing the work were:

A. H. Blessing	L. N. Montanino
R. C. Bryndle	J. M. Nowak
T. A. Lazzaro	E. J. White
D. Marshall	

This report was submitted and approved by H. Joseph Loftus.

The Bell Aerospace Report Number is 8651-928001.

This technical report has been reviewed and is approved.

Dr. D. George
Project Engineer

ABSTRACT

The objective of this evaluation was to investigate the feasibility of the powder rocket concept.

A series of rocket combustor tests were conducted at 500 and 900 pound thrust levels utilizing ammonium perchlorate/aluminum propellants. Eight 500 pound thrust fire tests were conducted to determine the effect of propellant variations on combustion. Particle size affected combustion stability with smoother combustion obtained with reduced particle size. Combustion oscillations of ±5 percent of mean chamber pressure at a frequency of 140 Hertz occurred utilizing 3 micron (X-65) Al and 20 micron AP which was the smoothest fire test. However, partial plugging of the AP injector occurred which was attributed to the agglomeration tendency of the finer AP. A test with AP containing 0.2 weight percent silica additive, improved the AP flow character but increased combustion oscillation level to ±38 percent of mean Pc.

Six 900 pound thrust fire tests were conducted with scaled up hardware utilizing a 50/50 by weight blend of 55 and 20 micron AP, with 3 micron (X-65) Al. Combustion oscillation amplitude ranged from ±18 to ±7 percent of mean chamber pressure.

Maximum specific impulse performance efficiency derived was 0.90 with the 900 pound thrust hardware and 0.93 for the 500 pound units.

A laboratory powder packing investigation was conducted to establish methods to maximize density of the AP powder. Some packing tests were performed with AP/Al mixtures. Results showed maximum packed density/particle density ratio of 0.77 for AP, and 0.75 for AP/Al mixtures.

CONTENTS

ILLUSTRATIONS

TABLES

TABLES (cont)

LIST OF ABBREVIATIONS AND SYMBOLS

A	Area (sq in.)
A*	Nozzle Throat Area (sq in.)
Al	Aluminum
AN	Ammonium Nitrate
AP	Ammonium Perchlorate
BeH_2	Beryllium Hydride
bell	Equivalent Nozzle Length Expressed in Percent of 15° Conical Nozzle
$BKNO_3$	Boron Potassium Nitrate
BN	Boron Nitride
BTU	British Thermal Unit
c*	Characteristic Velocity (fps)
C	Constant
CC	Cubic Centimeter
C_F	Thrust Coefficient
CH_2	Ethylene
CH_4	Methane
CPF	Chlorine Pentafluoride
D, d	Diameter (inches)
F	Thrust (pounds)
°F	Degrees Fahrenheit
Ft	Feet
G90	Graphite Formulation, Carborundum Co.

LIST OF ABBREVIATIONS AND SYMBOLS (cont)

h	Film Conductance (BTU/sq in.-sec°F)
H3	Aluminum Powder Grade, Valley Metallurgical Co.
H30	Aluminum Powder Grade, Valley Metallurgical Co.
HAP	Hydroxyl Ammonium Perchlorate
H	Enthalpy, BTU/lb
HNE	Hexanitroethane
H_2O	Water
I.D.	Inside Diameter (inches)
in.	Inches
Inj.	Injector
IR&D	Independent Research and Development
I_{sp}	Specific Impulse (lb-sec/lb)
K	Bed Flow Constant (lb/in.)
L	Length (inches)
L*	Characteristic Combustion Chamber Length (inches)
Lb	Pound
Mg	Magnesium
Ml.	Milliliter
N_2	Nitrogen
N_2H_4	Hydrazine
N_2O_4	Nitrogen Tetroxide
NOTSGELA	MHF-3 Gelled Fuel Containing 60 Percent by Weight Aluminum.

LIST OF ABBREVIATIONS AND SYMBOLS (cont)

Nu	Nusselt Number
O_2	Oxygen
O.D.	Outside Diameter (inches)
P	Pressure (psia)
Pc	Thrust Chamber Pressure (psia)
ΔP	Pressure Drop (psi)
PBCT	Polybutadiene Carboxyl Terminated
Pr	Prandtl Number
R	Gas Constant (feet/°R)
°R	Degrees Rankine
Re	Reynolds Number
Sec	Second
SEM	Scanning Electron Micrograph
SiO_2	Silicon Dioxide
T	Temperature
V	Volume
W	Weight (lb)
$\dot{W}$	Weight Flow Rate (lb/sec)
x	Packing Efficiency
X-65	Aluminum Powder Grade, Alcan Co.
ZrH_2	Zirconium Hydride

LIST OF ABBREVIATIONS AND SYMBOLS (cont)

ϵ	Nozzle Expansion Area Ratio
μ	Micron
η	Efficiency
ρ	Density (lb/cu ft)

1.0 INTRODUCTION

Previous powder rocket combustion effort was conducted under Bell Aerospace Independent Research and Development Program sponsorship, Reference 1. Low frequency combustion oscillations, which were encountered during initial testing, were reduced by substituting H3 type Al powder and methane fluidizing gas for H30/H3 blend Al and nitrogen gas.

The work reported herein involved three tasks:

1. Combustion and feed system evaluation
2. Powder packing evaluation
3. Analysis of experimental results

The original combustion test plan was modified to include 500 pound thrust hardware tests in order to select the powder sizes to be used to evaluate 900 pound thrust hardware. This approach was formulated because additional H3 Al was unavailable and a substitute Al was required. Additionally, the effect of reduced particle size AP and magnesium additive to Al merited investigation.

Previous laboratory powder packing investigations with Al were performed by Bell Aerospace, Reference 2. Consequently, contractual packing effort was directed principally toward maximizing the packing density of AP, with some work performed utilizing AP/Al mixtures.

The experimental results from this program and previous investigations were analyzed to assess the potential of the concept and identify technology areas which require further work.

2.0 SUMMARY, CONCLUSIONS, AND RECOMMENDATIONS

2.1 Summary

Design and fabrication of 900 pound thrust hardware which included two injector types and combustion chamber of three characteristic lengths; L* 65, 85, and 105 inches, was performed. Two single element injector configurations coaxial and mixing cup were selected. Combustion chambers consisting of graphite chamber and nozzle sections housed in stainless steel shells with bolted flanges were utilized. Similar 500 pound thrust hardware available from a previous program was used to evaluate combustion operation with various Al and AP powders preliminary to 900 pound thrust fire testing.

Cold flow and fire tests were performed flowing the powders from the piston type fluidized bed tank through a ball valve to the injector.

A series of eight 500 pound thrust fire tests were conducted. These included three variations of Al powder size, two different AP powder sizes, magnesium Al blends and silica additive to AP. Six 900 pound thrust fire tests were performed with variations in mixture ratio and characteristic chamber length using the same Al and AP for each test. The smoothest fire test which exhibited combustion oscillations of ±5 percent of mean chamber pressure at a frequency of 140 Hertz was attained by utilizing X-65 aluminum with 20 micron (nominal) ammonium perchlorate. Maximum specific impulse efficiency derived was 0.90 and 0.93 obtained with the 900 and 500 pound thrust hardware.

A correlation of AP powder cold flow characteristics with fire test flow data was exhibited. The Al fire test flow - ΔP characteristic was greater in ΔP and of decreased slope compared to the cold flow results. This caused operational difficulties in obtaining desired fire test conditions.

Laboratory scale packing tests were conducted with as-received AP powder using four different modes of blending for each of three particle size distributions. Utilizing the best blending mode and size distribution, packing tests with shape modified (rounded) particles were performed. Then the best blending mode, particle size distribution and shape powder was further evaluated with three anti-friction additives. Also, packing tests with AP/Al mixtures were performed. The highest packing efficiency (76.7 percent) attained in this investigation was obtained by combining powders in the premix mode in which the constituents are blended in a jar mill and with: large diameter ratio (20/400 micron), one constituent (400 micron) nominally round in shape, volume ratio of 50/70 fine/coarse, fumed silica as an anti-caking and flow additive, and surface treatment with fluoroethane. AP and Al powders were successfully blended by the premix mode to a packing efficiency of 75 percent, utilizing 50/50 weight percent 80/400 micron AP with H2 Al at an oxidizer fuel ratio of 2.0.

2.2 Conclusions

As a result of performing this work the following conclusions were made:

Powder propellant rocket engine feasibility was demonstrated by the performance of eight 500 pound thrust and six 900 pound thrust fire tests.

Low frequency combustion instability which was encountered appeared to be feed system coupled and forced by the heat-up and burning lag associated with the aluminum powder. Powder particle size affected stability with smoother combustion resulting with reduced particle size.

Partial plugging of the AP injector was attributed to the agglomeration tendency of the relatively fine AP. Addition of 0.2 percent by weight silica greatly improved the flow character but increased the combustion oscillation level to ±38 percent of mean Pc. The silica apparently coated the AP particles and inhibited deflagration processes.

Thrust chamber wall temperature measurements agreed with analytical predictions but throat values were somewhat higher. Variations in gas side film coefficient, hg, or wall thermal diffusivity could have caused higher than predicted throat temperatures. This was probably due to difference between the assumed and actual thermal diffusivity characteristic of the graphite wall material, which would have greater influence in the throat region than in the chamber due to the relatively higher heat flux.

Injection orifice discharge coefficients with powders were less than for water at equivalent flow rates. This is consistent with previous investigations which showed a reduced coefficient of discharge associated with the two phase solids - gas flow.

Partial plugging of the Al injector occurred during some cold flow and fire tests, with large, ~ 0.12 inch, Al particles evident in the orifice approach region. The particles were apparently formed in the loading system ball valve by compaction or extrusion of trapped powder during on-off cycling. This was alleviated by changing the loading procedure to eliminate valve cycling.

The premix mode was the most effective packing technique developed in this investigation for maximizing the density of ammonium perchlorate powders.

Fluoroethane and fumed silica additives improved packing efficiency of AP powders. A decreased packing efficiency was noted with boron nitride powder and with glass microballoons as additives.

Laboratory blending techniques can be successfully scaled-up without loss of packing efficiency.

2.3 Recommendations

Application studies should be conducted to establish systems in which the characteristics of powder propellants would be utilized to advantage compared to solid or liquid concepts.

Although AP/Al provided a readily available combination for concept feasibility investigations, higher performance fuels such as aluminum hydride and polyethylene should be fire tested.

Reverse flow or staged combustion injector configurations are recommended for future investigations. These injector designs are expected to enhance heat up and burning of the powders and consequently, improve combustion stability.

Efforts should be directed to spheroidize AP powders over a range of sizes to allow a wide latitude in blending, to improve packing efficiencies.

The evaluation of other anti-caking and flow additives should be continued.

3.0 TECHNICAL DISCUSSION

3.1 Combustion and Feed System Evaluation

3.1.1 Design Approach

3.1.1.1 Powder Selection

Graphic comparisons of specific impulse and density times specific impulse of typical liquid, solid and powder propellant combinations are presented in Figures 1 and 2. The specific impulse of powdered propellants is competitive with solid and liquid reactants, and the theoretical density times specific impulse is somewhat better. Effect of powder packing efficiency is shown on the latter figure which depicts the significance of packing on effective propellant density. Liquid propellant density decrease resulting from bulk temperature extremes of 77 to 200°F are shown.

In addition, powders offer a combination of flexibility and storability advantages which are not completely achieved with liquids, solid and hybrid rockets. For example, powder flows are easily throttled and their mass flow rate appears to be insensitive to environmental temperature extremes.

AP and Al were selected for this feasibility investigation because of availability and since these propellants are widely used in solid rockets. Thermochemical shifting equilibrium performance for AP/Al combustion is presented in Table I.

Powder particle size selection was influenced by combustion and packing considerations. Maximum combustion efficiency for a given residence time is obtained with small particle size while maximum packing density is achieved with mixture of mostly large with some small particles. Combustion of Al is rate controlling which constrains fuel particle size to diameters of 40 microns or less while the deflagration of AP in 7000°R gases was expected to be relatively fast, so oxidizer particle size to diameters of 400 micron was considered. Spherical aluminum powder of 3 micron (nominal) diameter was selected based on combustion results from previous investigations, Reference (1). Also from this previous work 55 micron (nominal) diameter AP was selected based on powder cold flow tests.

These and other powders used during this program were characterized to determine particle size distribution (See Table II).

3.1.1.2 Injector

Powder rocket injector design criteria and techniques for powder propellants are generally similar to those utilized for liquid propellant injectors. However, since the powders are injected in particulate form propellant atomization is not required. The powder injector for this application delivers a uniform flow of

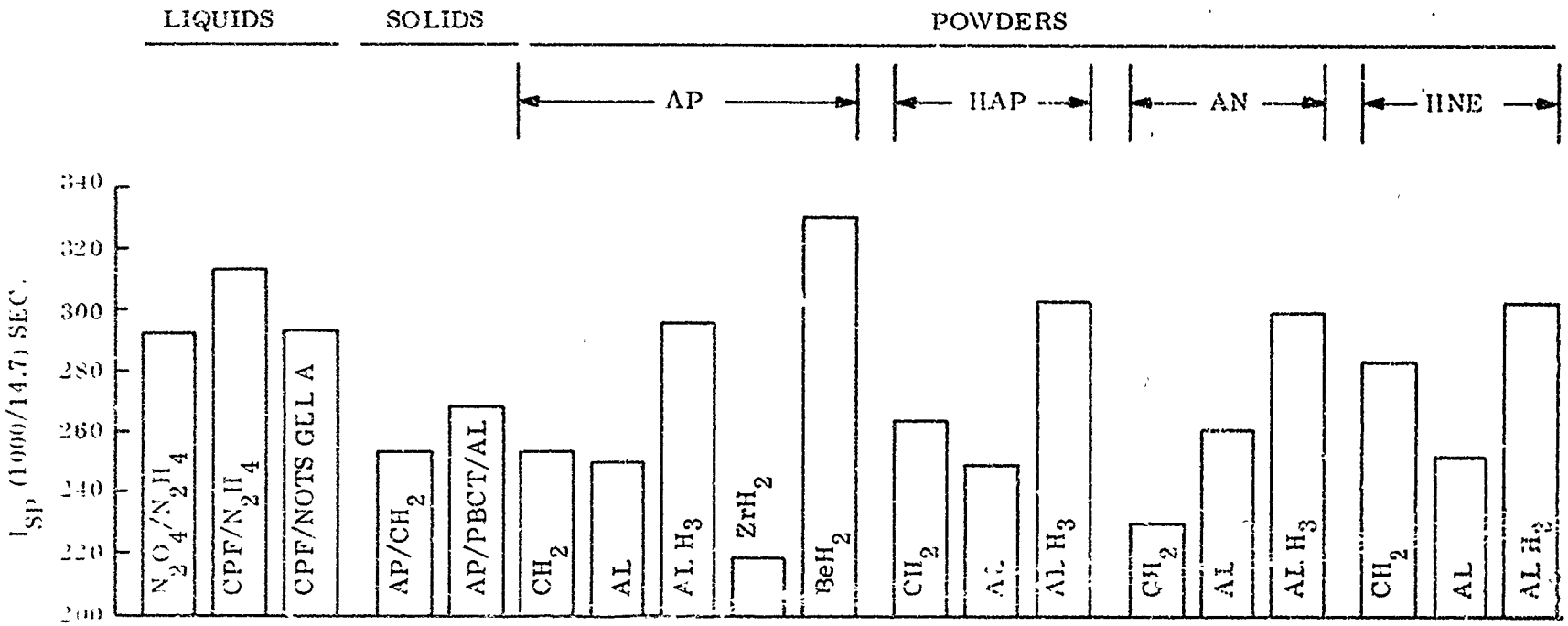

Figure 1. Theoretical Specific Impulse Comparisons

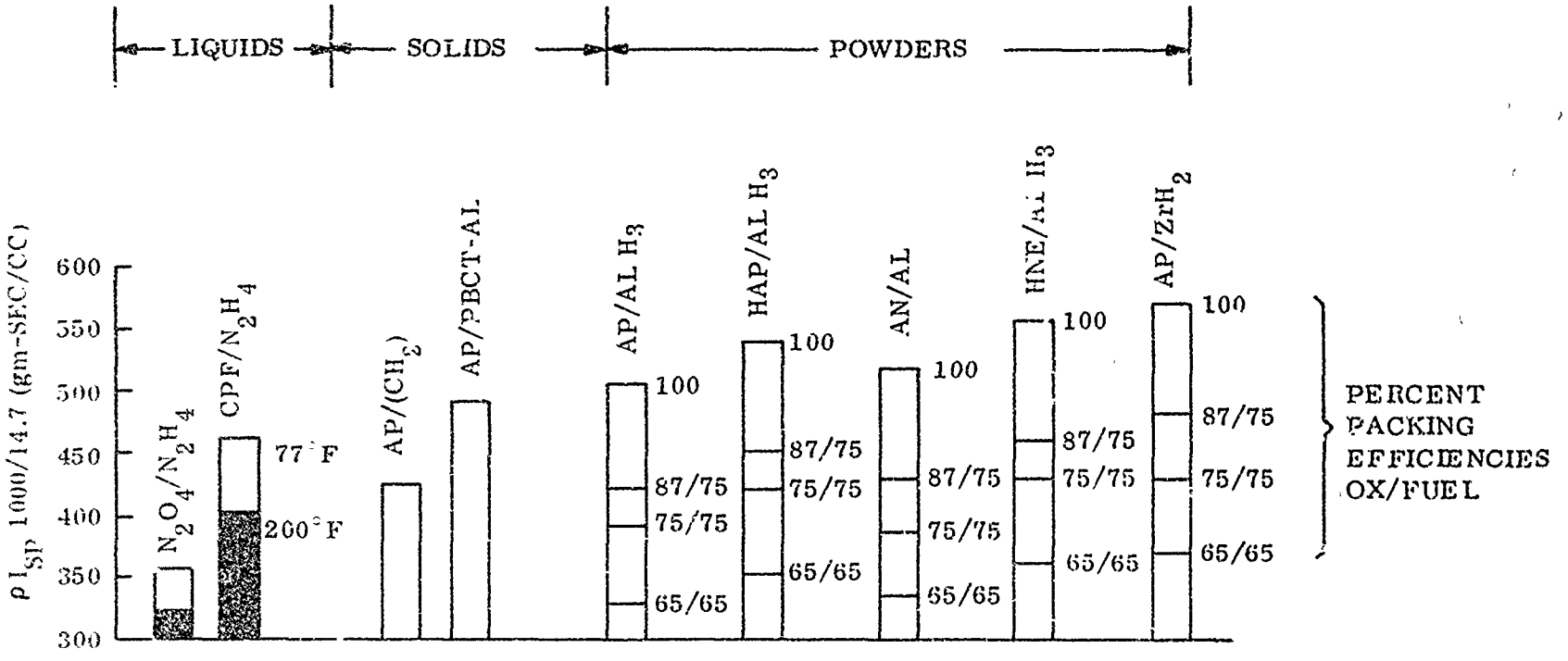

Figure 2. Theoretical Density Impulse Comparisons

TABLE I

AP/AL THEORETICAL PERFORMANCE PARAMETERS

Pc = 500, Shifting Equilibrium

Mixture Ratio O/F	Specific Impulse $\epsilon = 6.0$ Lb-Sec/Lb	Character Velocity Ft/Sec	Combustion Temperature °R
3.5	254	4760	6911
3.0	255	4791	7150
2.5	255	4818	7399
2.0	254	4763	7621
1.5	249	4661	7720
1.2	242	4508	7587
1.1	238	4431	7481
1.0	234	4359	7311
0.9	227	4241	7040
0.8	218	4080	6612

TABLE II

POWDER CHARACTERISTICS

Powder	Nominal Particle Size - μ	Distribution Wt % Above Stated Size - μ		
		10%	50%	90%
AP	55	66	38	16
AP	20	44	17	4.2
AL	5 (H5)	22	9.6	3.7
AL	3 (H3)	12	6	3
AL	3 (X-65)	12.9	7.4	3.8

AP and Al particles to the combustion zone. Combustion of Al is the rate limiting process in the burning model in which the AP decomposes exothermically producing thermal energy and oxidants for heat up and combustion of Al. Injector manifold design was more critical due to the two phase solids/gas mixture.

For this program the injector designs were based on experience gained from the previous program and were scaled-up versions to accommodate propellant flow rate increases for a 900 pound thrust chamber. Two basic single element injector configurations, coaxial and mixing cup, were selected for evaluation as shown in Figure 3. The coaxial unit consisted of a central AP orifice containing a vortex insert, surrounded by an annular Al element. The mixing cup injector contained a center Al orifice with a vortex insert and a tapered tangential AP orifice. These orifices exited into a throated mixing cup prior to injection into the combustion chamber. Both injectors avoided manifolding between the feed lines and orifice approach to eliminate flow area expansion, and subsequent gas/powder separation determined to be a problem area on the previous program.

A summary of the injector design parameters for the two configurations is presented in Table III. Also shown in the table are the design parameters for the previous program coaxial injector, which was utilized for powder evaluation during the initial portion of the test program. The coaxial annulus gaps for Al injection were based on a minimum of 0.030 inch based on previous orifice cold flow test. The 900 pound Al coaxial injection area was sized to allow for increased fuel side ΔP and injection velocity, determined to be beneficial based on previous testing. The same oxidizer velocities were maintained. The fluidized powder density values used for calculation of propellant velocities and pressure drops were 42.7 lb/cu ft for AP and 73.5 lb/cu ft for Al. Injection velocities for the Al were in the order of 45-70 ft/sec for both injectors, and the AP ranged from 80 ft/sec in the coaxial vortex center to 140 ft/sec in the tangential premix injector.

The injectors were fabricated principally of 300 series stainless steel with the faceplate, which was exposed to the combustion chamber, made from A-200 nickel. A bolted injector-chamber flange joint with Viton O-rings was used.

3.1.1.3 Thrust Chamber

Design data used for sizing the thrust chamber for this program are presented in Table IV. The chamber assembly provides a delivered sea level thrust of 900 pounds while using powdered AP/Al at an optimum mixture ratio of 2.5 and a chamber pressure of 300 psia. The assembly can be seen in Figure 4.

The assembly consists of graphite combustion chamber and nozzle section liners housed in stainless steel shells. The nozzle and chamber sections are assembled with bolted flanges. Viton O-rings are used to provide seals between the graphite liners and stainless steel housings, chamber-to-nozzle joint and injector-to-chamber joint. Two combustion chamber pressure ports are located at the nozzle entrance station. Combustion residence time variation can be achieved

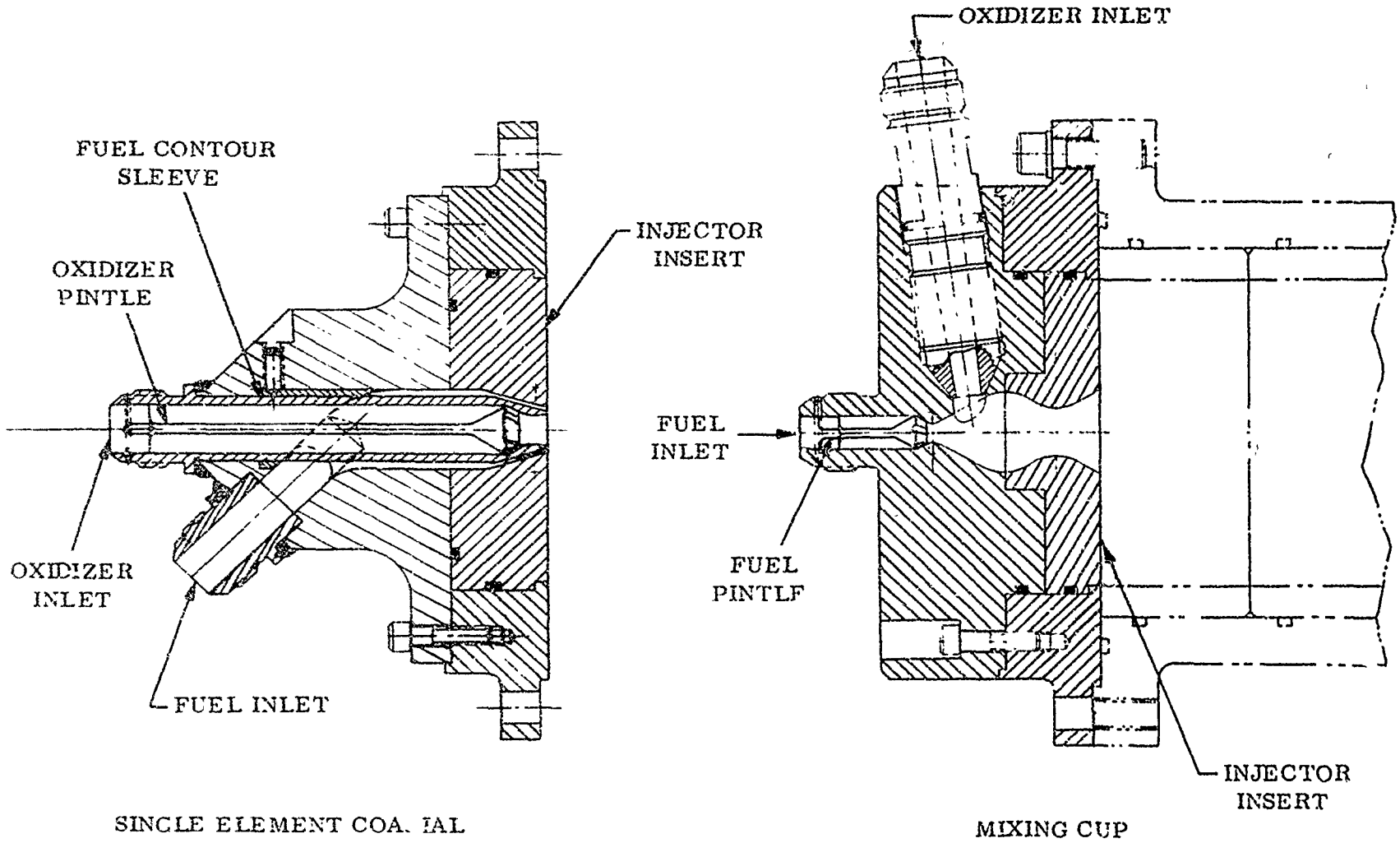

Figure 3. Powder Rocket Injector Assemblies

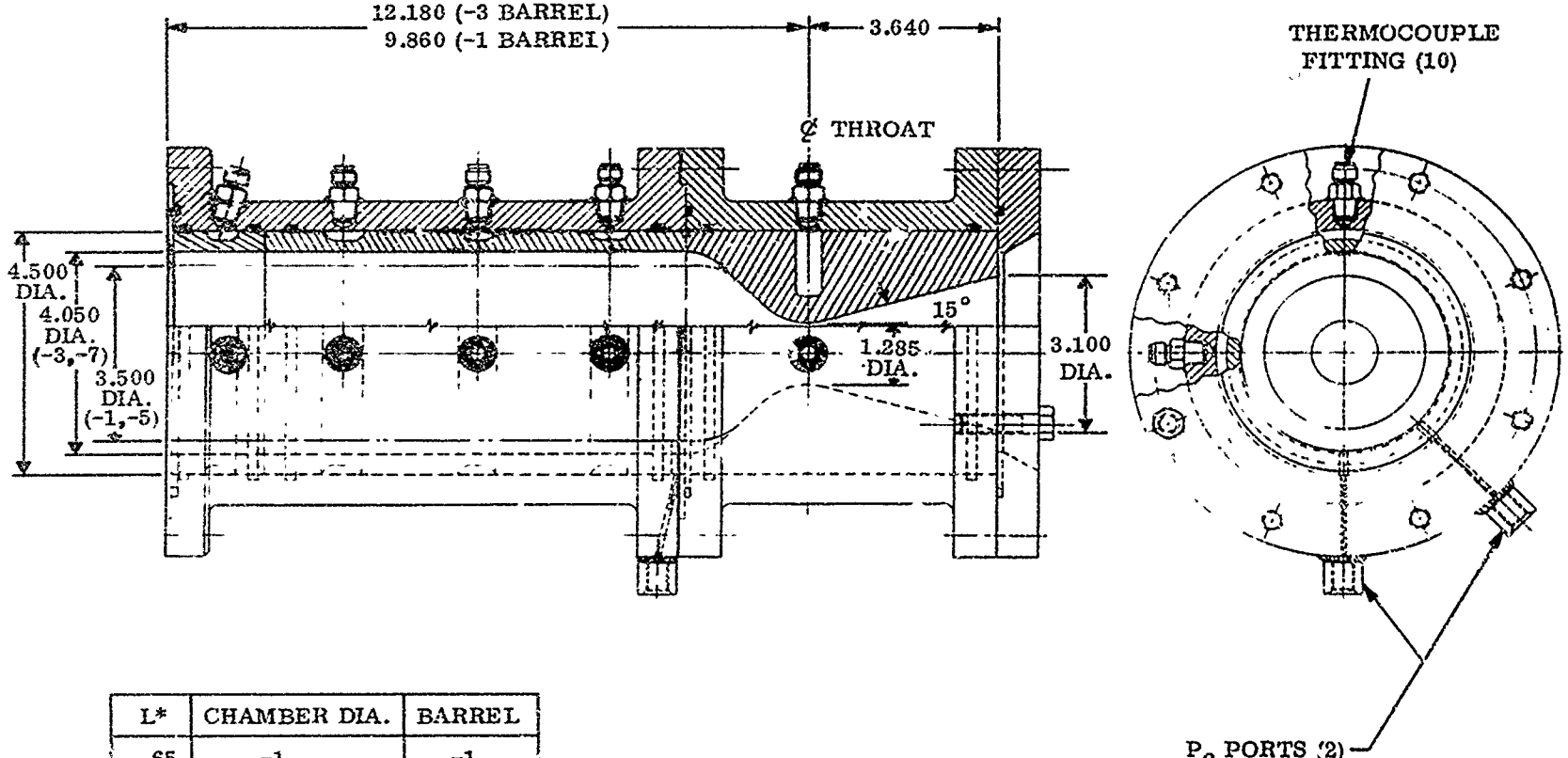

L*	CHAMBER DIA.	BARREL
65	-1	-1
85	-3	-1
85	-5	-3
105	-7	-3

Figure 4. Powder Rocket Combustion Chamber Assembly

TABLE III

INJECTOR DESIGN PARAMETERS

CONFIGURATION	ANNULUS (FUEL)						CENTER (OXIDIZER)						
	I.D. (in.)	O.D. (in.)	Gap (in.)	Inj. Area ($in.^2$)	Inj. Angle (°)	Inj. Vel. (ft/sec)	No. Slots	Slot Angle (°)	Slot Width (in.)	Slot Height (in.)	Total Slot Area ($in.^2$)	Slot Velocity (ft/sec)	Pintle Holder Exit Dia. (in.)
Coaxial 8651-473110	0.530	0.590	0.030	0.0525	15	47	6	30	0.137 Avg.	0.140	0.134	80	0.400
IR&D Unit Coaxial	0.399	0.458	0.030	0.0397	15	31	3	30	0.220	0.083	0.067	80	0.281

CONFIGURATION	TANGENTIAL ORIFICE (OXIDIZER)				CENTER (FUEL)						
	Dia. (in.)	Area ($in.^2$)	Cone Inj. Angle (°)	Inj. Velocity (ft/sec)	No. Slots	Slot Angle (°)	Slot Width (in.)	Slot Height (in.)	Total Slot Area ($in.^2$)	Slot Velocity (ft/sec)	Pintle Holder Exit Dia. (in.)
Mixing Cup 8651-473101	0.308	0.0744	7.5	143	5	30	0.086	0.086	0.037	67	0.265

Propellants	$AP(NH_4 CLO_4)/AL$
Propellant Flow Rate, total lb/sec	4.41
Mixture Ratio O/F	2.50
55 μ Oxidizer (AP) density (1), lb/ft^3	42.7
3 μ Fuel (AL) density (1), lb/ft^3	73.5
Injection orifice pressure drop - psi	50 - 200

(1) Includes fluidization gas.

TABLE IV

THRUST CHAMBER DESIGN PARAMETERS

Propellants	NH_4CLO_4/AL
Propellant Flow Rate, Total, Lb/Sec	4.41
Mixture Ratio O/F	2.50
Thrust S.L. Lb	900
Combustion Chamber Pressure, Psia	500
I_{sp}, Specific Impulse, Lb-Sec/Lb (Sea Level)	204 (1)
C*, Characteristic Velocity, Ft/Sec	4580 (1)
C_F, Thrust Coefficient	1.44 (1)
Performance Efficiencies, ηI_{sp}, ηC^*, ηC_F	.89, .95, .94
Chamber Diameter, In.	3.50, 4.05
Throat Diameter, In.	1.265
Exit Diameter, In.	3.100
Expansion Area Ratio, ϵ	6.0
Nozzle Contour, % Bell	100
Chamber Length (Inj. to Throat), In.	9.90, 12.2
Chamber Characteristic Length, In.	65, 85, 105
Cooling Mode	Heat Sink

(1) Expected Delivered Values.

by changing combustion volume, L*, and by varying chamber diameter and/or chamber length with the respective graphite liners. The design rated residence time for complete combustion was 4 milliseconds with a corresponding 85 L* chamber characteristic length (12.2-inch chamber length and 3.50-inch chamber diameter). The L* and residence time variations possible with the graphite liners are 65 L* and 3 milliseconds, and 105 L* and 7 milliseconds.

Included on the chamber and nozzle housings are 10 thermocouple fittings to allow for measurement of outer graphite liner temperatures. The graphite liners have reduced wall thickness sections of 1/4 inch in the chamber and 1/2 inch at the throat, corresponding to the thermocouple fitting locations, see Figure 4.

Thermal analysis results were the basis for wall thickness reductions made to obtain higher temperature levels during fire test.

Thermal Analysis

A thermal analysis of the thrust chamber was performed in order to predict wall temperature, heat flux and total heat loss. The computation of the gas side heat transfer coefficient considers comressibility effects, recombination of highly dissociated gas species and variable transport properties in the boundary layers. A modified form of the Colburn equation was used, wherein the properties are evaluated at the Eckert reference enthalpy (Reference 3), according to the following correlation equation:

$$(Nu^*) = C(Re^*)^{0.8} (Pr^*)^{0.4}$$

where Nu = Nusselt Number

Pr = Prandtl Number

Re = Reynolds Number

and the Superscript* refers to the reference enthalpy conditions.

For fully developed turbulent pipe flow the value of C is 0.026. It was found by investigation e.g., Schacht, Quentmeyer and Jones, Reference 4, that test firings could be correlated by varying the value of C with area ratio being a minimum at the throat, as shown in Figure 5. The correlation constant used by Bell Aerospace has been extended to larger area ratios.

In Reference 3 it is recommended that the transport properties appearing in the correlation equations be evaluated at a temperature corresponding to a reference enthalpy given by the equation:

$$H^* = 0.5 (H_s + H_w) + 0.22(Pr^*)^{1/3}(H_c - H_s)$$

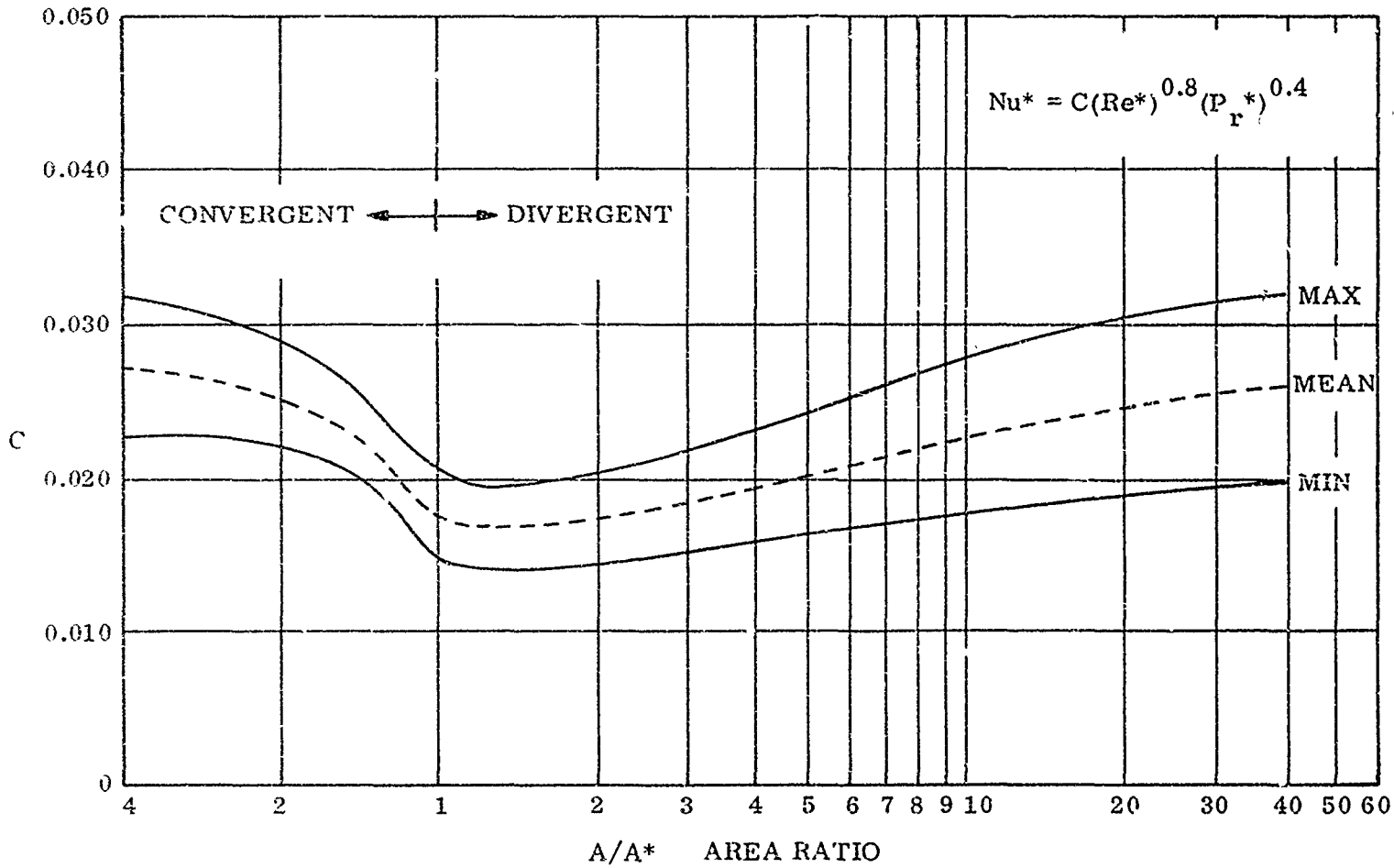

Figure 5. Gas Film Coefficient Distribution

with	H	=	enthalpy, BTU/lb	Subscript	s	=	static
	Pr	=	Prandtl Number		w	=	wall
					o	=	total

Flow properties at any axial station in the nozzle are computed using compressible flow relations.

Thermal response of the chamber wall was estimated assuming the wall to be a thick cylindrical slab heated on the one side and insulated on the other side. Graphical analytic solutions for this condition were utilized, Reference 5. Using the estimated value of the heat transfer coefficient at the throat, hg, of 0.00343 BTU/sq in.-sec°F the temperatures at the inner and outer surfaces in the throat and chamber were computed for both copper and G-90 graphite. The thermal properties and heat transfer coefficients utilized are shown in Table V. Computed temperatures at the end of a 2-second firing are shown in Table VI. It is evident that copper would be well in excess of its melting point at the throat, however, it would be satisfactory in the chamber. The graphite temperatures are seen to be higher at the inner wall, however the temperatures at the outer surface would be quite low, ie, less than 400°F. In order to obtain increased temperature level during a test firing, it would be necessary to either fire the chamber for a longer duration or reduce the thickness of the wall where thermocouples are placed. The latter approach was implemented in both the chamber and throat. Locally, walls of the chamber and throat were decreased to thicknesses of 0.25 and 0.5 inch, respectively. Predicted temperatures for the reduced thickness are also shown in Table VI.

Total heat rejected by the hot gases to the chamber during the firings were determined by integrating the heat flux over the surface area. The heat flux, total heat and specific heat rejection, have been computed at both the start of a firing with ambient wall temperature and at the 2-second point as shown in Table VII.

Energy loss due to heat transfer may be assessed by comparing the predicted values with the values obtained from shifting equilibrium thermochemical calculations shown in Table VIII.

3.1.1.4 Igniter

The ignition of powdered propellants requires considerations applicable to both liquid and solid propellants. Ignition of AP/Al requires sufficient thermal energy to initiate decomposition of AP, at approximately 300°F, which in turn provides heat and oxidants for Al combustion, at approximately 1100°F. In order to achieve these conditions it was desirable to have an igniter that produces high temperature products at relatively low chamber pressure.

For this program a pyrotechnic igniter was developed based on a scaled-up version of a similar igniter developed for the previous program. The igniter contained a S-67 (DuPont) squib, 4 grams of smokeless powder (No. 4895), and 12.4

TABLE V

THRUST CHAMBER WALL THERMAL PROPERTIES
AND HEAT TRANSFER COEFFICIENTS

Parameter	Copper	Graphite G-90
Conductivity, BTU-In./Ft^2Hr°F	2500	250
Density, Lb/$In.^3$	0.323	0.0682
Specific Heat, BTU/Lb°F	0.093	0.45
Thermal Diffusivity, $In.^2$/Sec.	0.161	0.0157

GAS SIDE HEAT TRANSFER COEFFICIENTS

hg-BTU/$In.^2$-Sec°F

Throat	0.00343
Chamber	
4.05 Dia.	0.00077
3.5 Dia.	0.00104

TABLE VI

THRUST CHAMBER WALL TEMPERATURE DISTRIBUTION
AFTER 2.0 SECONDS

Region	T_{inside} °F	$T_{outside}$ °F	t_{wall} In.
Throat			
Copper	2430	140	1.818
G-90	4260	70	1.818
G-90	4430	344	0.500
Chamber			
D - 4.05 In.			
Copper	997	778	0.425
G-90	1800	350	0.425
G-90	1930	900	0.25
D - 3.5 In.			
Copper	960	490	0.700
G-90	2110	140	0.700
G-90	2270	1040	0.25

TABLE VII

THRUST CHAMBER HEAT REJECTION

Region			Time Sec.	Surface Area $In.^2$	Heat Flux $BTU/In.^2$-Sec	Heat Rejection BTU/Sec	Specific Heat Rejection BTU/Lb
Throat			0	9.38	23.5	221	50
			2	- -	9.2	87	20
Chamber	L*	Dia. In.					
-1	65	3.5		82.4			
			0		6.74	559	127
			2		4.74	390	89
-3	85	4.05		95.5			
			0		5.32	508	115
			2		3.98	380	86
-5	85	3.5		107.7			
			0		6.74	725	165
			2		4.74	510	116
-7	105	4.05		124.8			
			0		5.32	663	151
			2		3.98	500	114

TABLE VIII

EFFECT OF ENERGY LOSS ON THRUST CHAMBER PERFORMANCE
NH_4C10_4/AL
Pc = 500

Energy Loss BTU/Lb	Parameter	Mixture Ratio - O/F		
		2.0	2.5	3.0
0				
	C*	4818	4791	4768
	I_{sp} at S.L.	228.7	228.5	227.4
100				
	C*	4717	4743	4739
	I_{sp}	225.8	226.7	226.2
200				
	C*	4677	4690	4689
	I_{sp}	223.5	224	223.8
300				
	C*	4621	4641	4639
	I_{sp}	221.3	222.1	220.4

grams of $BKNO_3$ pellets. These constituents were assembled in a cloth bag and installed through the throat to the injector end of the combustion chamber. This igniter produced 20-25 psia chamber pressure with a burn period of 0.150 to 0.200 seconds.

3.1.2 Test Setup and Procedure

The test program was conducted at Test Cell 1CE2. A schematic of the propellant feed system and thrust chamber assembly including the location of all test measurements is presented in Figure 6.

The thrust chamber assembly was mounted on a flexure supported thrust stand with the injector placed between the chamber and thrust plate. The stand has the capacity to test engines to 20,000 pounds thrust, but for test on the order of 1,000 pounds thrust a 2,000 pound load cell is installed. Standard pressure, temperature, thrust measurements were utilized on the stand to determine the chamber pressure, liner temperatures and performance of the thruster.

Specific impulse and characteristic velocity were the primary performance parameters derived from fire test measurements. In addition, the temperature response of the graphite liner at 4 stations in the chamber section and one at the nozzle throat was measured.

Also, exhaust particulate samples were collected utilizing an Air Force furnished exhaust sampler. Chemical analyses of the samples were performed.

Cold flow of the injector and feed system was conducted by removing the chamber and attaching a special test fixture to the injector. The fixture consisted of a flange; line, pressure and force transducers; a Pc simulation orifice; and a powder receiver. This receiver allows the fluidizing gas to vent but retains the solid particles. Fluidization gas flow rates were measured using turbine-type flowmeters.

The powder propellants were fed from separate piston-type positive expulsion fluidized beds. These beds or tanks were mounted on the thrust stand and connected to the injector with short fixed lines through a single ball-type flow control valve. The fluidized powder tank assembly is shown in Figure 7. The gas actuated piston follows the bed during powder expulsion and its displacement was measured with a potentiometer. Correlation of the bed displacement and solids flow rate from cold flow tests was used to obtain mass flow rate during fire tests. Powder was transported by introducing fluidizing gas into the bed via the piston rod and a porous plate mounted on the piston face. This porous plate distributes the gas uniformly and also prevents powder backflow during fill and vent operations.

The fluidization gas was introduced separately from the piston actuation gas, which in turn is prevented from entering the powder bed by O rings on the piston. When N_2 is used for fluidizing, the fluidization gas regulators were fed from

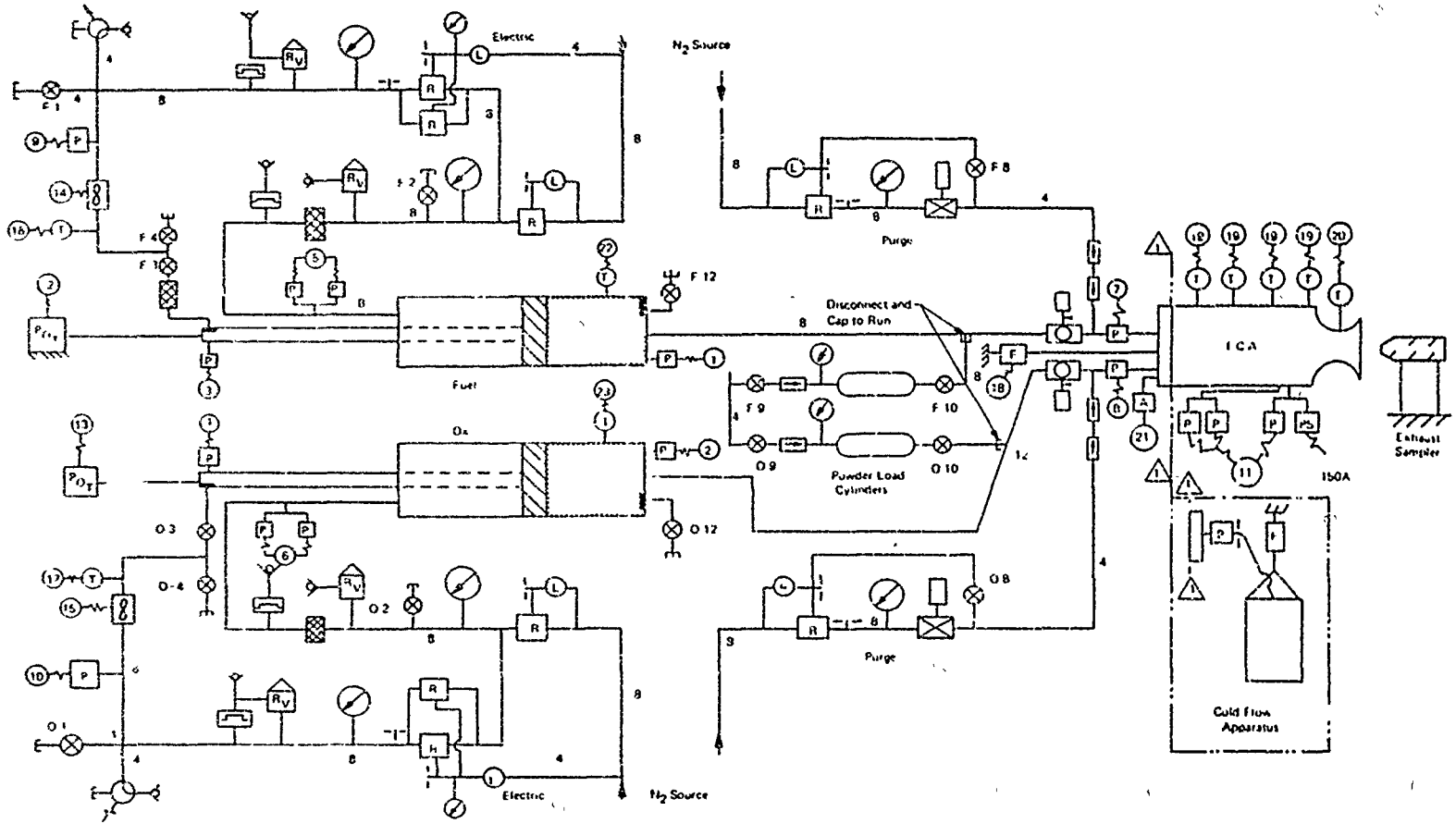

Figure 6. Schematic - Powder Propellant Test Facility 1CE-2

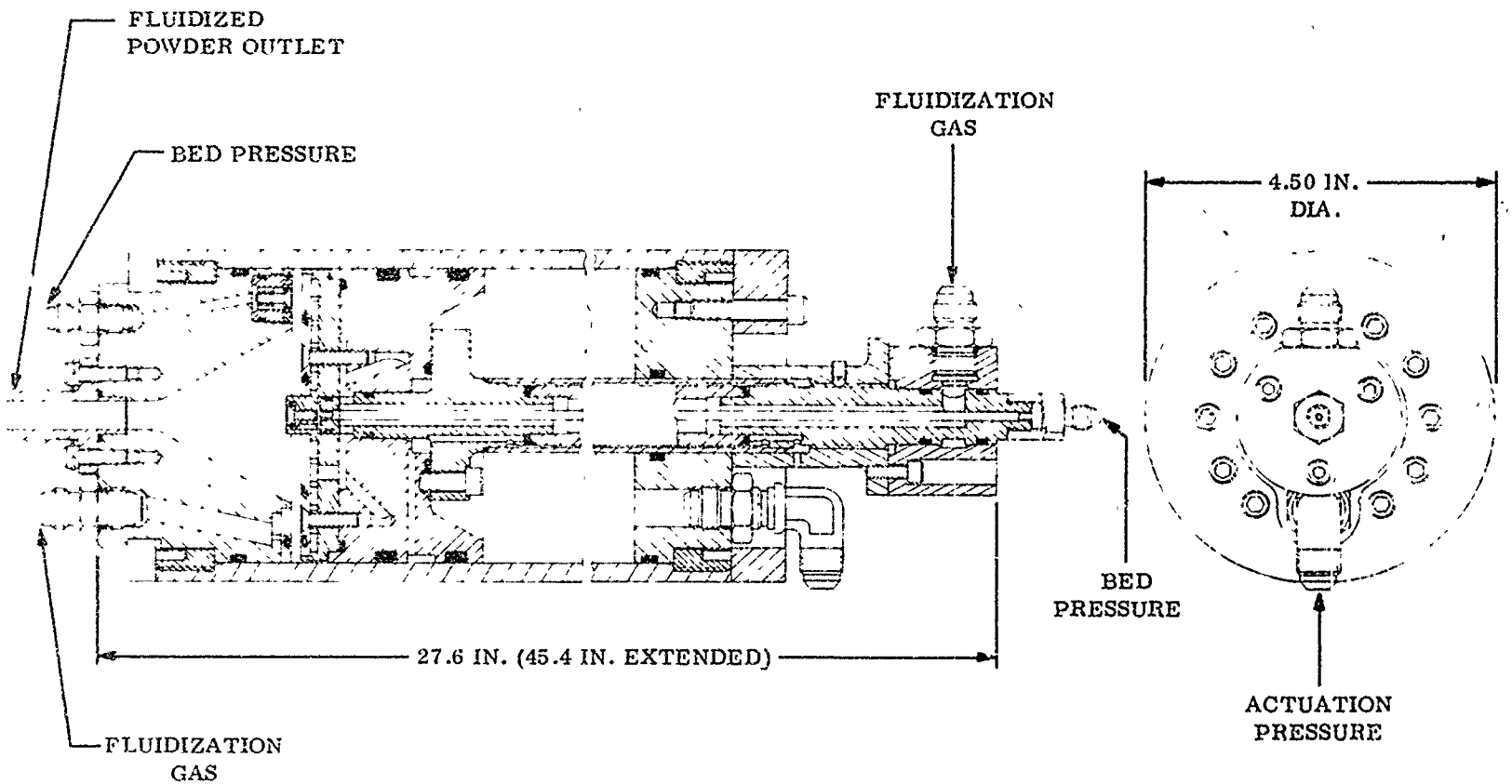

Figure 7. Powder Fluidization Unit Assembly

the N_2 actuation gas regulator to provide positive control of the piston differential pressure. When reactive gas O_2 was used for AP fluidization separate regulators were used for piston actuation. For this program, fluidization gas used was CH_4 for Al, N_2 and O_2 during 500 and 900 pound thrust tests, respectively for AP. The gas pressure in the bed at the piston face was measured by a transducer on the end of the piston rod. Bed pressure at the outlet end of the tank was measured by a standard pressure transducer and provision was also made in the tank to either introduce or vent fluidization gas at the outlet end.

Feed pressures in the lines just upstream of the injector were measured by in-line pressure transducers. The powder flow passes through the head of the transducer where the sensing diaphragm is one wall of the flow passage. Standard gas purge systems were provided just downstream of the valve to expel the powder in the feed line to the injector at shutdown.

The powder propellants were loaded into the run tanks by manually filling separate load cylinders and fluidizing the powder into the run tanks. To do this, the run tank fluidization ports were vented, allowing the fluidizing gas to escape through the porous plates while the powder was retained in the tank. The load lines were then disconnected and capped prior to thrust chamber firing.

Test firings were conducted in the following manner. Preparatory operations include instrumentation checkout and powder propellant loading. The fluidized bed tanks were pressurized with fluidization gas to a predetermined value. Piston actuation pressure was maintained at 100 to 150 psi above the bed pressure. Tank pressure was established by summing the expected combustion pressure, and injector and feed system pressure drops derived from cold flow tests. After the bed and piston actuation pressures were adjusted to the run values, the fire test was initiated according to the following sequence:

1. Fuel stand valve actuated.
2. Oxidizer stand valve actuated.
3. Igniter squib energized.

The oxidizer valve opening was delayed to give a 0 to 0.020 second fuel lead on start. An igniter squib time delay of about 0.100 second was programmed to allow for valve opening and line filling, before propellant entry into the combustion chamber. All tests were conducted with a CH_4 gas/AP start phase of about 0.300 second duration after which the Al powder was introduced. The CH_4 gas was introduced downstream of the Al flow control valve. The CH_4 flow control valve was closed about 0.100 second after introduction of Al powder.

Shutdown was accomplished by de-energizing the propellant valves. The fuel valve closes first while the oxidizer valve was delayed to provide about 0.05 second lag. This tends to eliminate the accumulation of unreacted aluminum on the chamber and nozzle surfaces.

The data acquisition system consists of varied types of end instruments required for obtaining flow rates, temperature, pressure, thrust, events and related test parameters. A listing of the parameters, shown in the schematic, range of instruments used and associated measurement error are presented in Table IX. The measurement uncertainty of the derived specific impulse and characteristic velocity parameters was established by statistical combination of the individual measurement errors shown in the table. Powder mass flow error of ±3.3 percent was determined from previous cold flow data (Reference 1). The predicted error associated with the performance parameters are:

Specific Impulse	2.5 Percent
Characteristic Velocity	2.4 Percent

The sensors used are of two main groups, the self generating pickups such as inductive, thermoelectric, and piezoelectric, and a second type requiring excitation voltage, namely; voltage dividers, potentiometric, strain gage bridge, and variable differential transformers. The sensor output signals may be split and recorded simultaneously on two or more of four principal data acquisition systems used to record test data, namely, a Beckman system, FM tape recorder, oscillograph and graphic recorder. For this program, the Beckman, oscillograph and graphic systems were used. Brush recorders were used in the test cell to monitor setups. The parameters required for determining performance characteristics of the engine were recorded on the Beckman system.

3.1.3 Test Results

Prior to initiation of fire tests with the 900 pound thrust hardware, a series of powder stability evaluation fire tests were conducted with the 500 pound thrust hardware. This was necessary due to lack of supply of the original H3 Al formerly used and found to provide the smoothest combustion during initial 500 pound testing. The vendor, Valley Metallurgical could only supply H5 Al, with a mass median diameter of 9.7 micron compared to 6.0 micron for the H3 Al powder.

Prior to fire test a series of injector cold flow tests were conducted, as summarized in Table X, to establish injector and fluidized bed calibration powder mass flow data for use in fire test setup.

The H5 Al powder would not pass through an 80 mesh screen, routinely used for processing Al powder prior to loading. Initial cold flow tests resulted in plugging of the fuel annulus in the coaxial injector. Small fibrous particles were observed. Additional powder was then screened (20 mesh) and satisfactory flows were achieved.

Fire test data are summarized in Table XI. Operating conditions, performance, stability and feed system parameters are included in the table. Performance parameters were omitted during tests in which, combustion oscillation

TABLE IX

POWDER ROCKET INSTRUMENTATION

No.	Symbol	Parameter	Qty	Recorder				Range	Measurement Uncertainty (3 σ, 90% UCL) (1)
				Beckman		Oscillo-graph	Brush		
				A	B				
1	FTOP	Fuel Tank Outlet Pressure	1	X		X	X	750 psia	1.1
2	OTOP	Oxidizer Tank Outlet Pressure	1	X		X	X	750	1.1
3	FTPFP	Fuel Tank Piston Face Pressure	1	X				750	1.1
4	OTPFP	Oxidizer Tank Piston Face Pressure	1	X				750	1.1
5	FPAP	Fuel Piston Actuation Pressure	2	X		X		1000	1.0
6	OPAP	Oxidizer Piston Actuation Pressure	2	X		X		1000	1.0
7	FFP	Fuel Feed Pressure	1	X		X	X	750	1.1
8	OFP	Oxidizer Feed Pressure	1	X		X	X	1000	1.1
9	FFLP	Fuel Fluidization Line Pressure	1	X				750	1.1
10	OFLP	Oxidizer Fluidization Line Pressure	1	X				750	1.1
11	TCPC	Thrust Chamber Pressure	3	X		X	X	750 psia	1.0
12	POTF	Fuel Tank Piston Displacement	1	X			X	24 inches	0.5
13	POTO	Oxidizer Tank Piston Displacement	1	X			X	24 inches	0.5
14	WFFG	Fuel Fluidization Gas Flow Rate	1		X	X		0.01-0.1 lb/sec	1.7
15	WOFG	Oxidizer Fluidization Gas Flow Rate	1		X	X		0.1-0.25 lb/sec	1.7
16	TFFG	Fuel Fluidization Gas Temperature	1	X				0-100 F	± 2 F
17	TOFG	Oxidizer Fluidization Gas Temperature	1	X				0-100 F	± 2°F
18	F	Thrust	2	X		X	X	2000 lb	1.0
19	TLSC	Chamber Liner Skin Temperature	8		X			0-1000°F	± 4°F
20	TLSN	Nozzle Liner Skin Temperature	2		X			0-1000°F	± 4°F
21	AX	Axial Acceleration	1			X	X	2000 g (2)	± 3.0
22	FTST	Fuel Tank Skin Temperature	1		X			0-100°F	± 2°F
23	OTST	Oxidizer Tank Skin Temperature	1		X			0-100°F	± 2°F
		Fire				X			
		Shutdown				X			
		Igniter Squib				X			
		Oxidizer Stand Valve Power				X			
		Fuel Stand Valve Power				X			
		Oxidizer Stand Valve Open				X			
		Fuel Stand Valve Open				X			
		Thrust Chamber Pressure				X			
		Time Code				X			

(1) In percent unless otherwise noted.

(2) Assumes 2000 g is peak to peak.

TABLE X

POWDER COLD FLOW TEST SUMMARY

Test No ICE-	Inj. Conf.	Propellants: Fuel	Propellants: Oxidizer	W lb/Sec	Pc Psia	FFSP Psia	FTPFP Psia	FTOP Psia	FFP Psia	ΔP_{Line} FTOP − FFP	$\Delta P_{inj.}$ FFP − Pc	$\Delta P_{Sys.}$ FTOP − Pc	OPAP Psia	OTPFP Psia	OTOP Psia	OFP − Psia	ΔP_{Line} OTOP − OFP	$\Delta P_{inj.}$ OFP − Pc	$\Delta P_{Sys.}$ OT − Pc	Remarks
98A	Coax-	5μ Al	-	0.96	490	771	607	601	553	48	63	111	-			-	-	-	-	Results questionable since injector plugging occurred, fibrous particles in annulus
98B	500 lb		-	0.88	391	685	512	507	461	46	70	116	-	-				-		
98C			-	0.68	267	579	414	412	373	39	106	145	-	-		-		-		
98D			-	0.95	562	905	763	757	708	49	146	195		-				-		
99A			-	0.73	312	578	400	396	356	47	44	85	-	-			-	-		Results satisfactory - Used screened powder.
99B			-	0.91	488	780	603	591	551	40	63	103	-			-				
99C		5μ Al		0.94	558	870	708	700	654	46	96	142	-	-		-				
105A		--	20μ AP	1.97	401		-	-	-	-		-	826		645	494	131	93	244	Unsatisfactory - Powder bulk
106		--	20μ AP	1.75	389		-	-	-	-		-	829		685	551	134	162	296	Satisfactory-Vac. dried powder.
108A	Coax-	--	20μ AP +	2.08	462		-	-	-	-	-	-	804		671	605	65	143	208	Evaluate SiO_2 to prevent agglomeration.
108B	500 lb		0.2 SiO_2	1.85	481	-	-	-	-	-		-	745		645	605	40	121	164	
																	(OTPFP-OFP)		(OTPFP-Pc)	
113A	Coax.-	-	AP	3.20	489		-	-	-		-	-	855	710		660	50	171	251	Piston ΔP decay below 100 psi during flow.
113B	900 lb	--	50/50-	2.96	453	-	-	-	-	-	-		774	670	-	610	60	157	217	
113C		--	20μ/55μ	3.06	422	-	-	-	-	-	-	-	718	633	-	560	73	138	211	
113D		-	(N_2 fluid)	2.95	ATM.	-	-	-	-	-	-	-	415	231	-	179	52	164	216	Movies to ATM.
114A		--		2.87	480		-	-	-	-	-	-	829	704	-	641	63	161	224	Increased piston ΔP.
114B		--		2.54	445		-	-		-		-	814	632	-	578	54	133	187	
115A		X-65 Al	-	1.77	593	892	760	726	665	61	72	133	-	-	-	-	-	-	-	Initial flows with X-65.
115B				1.51	523	840	685	656	594	62	71	133	-	-		-	-	-	-	
115C			-	1.38	428	734	576	545	491	54	63	117	-	-	-	-	-	-	-	
116A			-	1.26	461	786	615	600	541	59	80	139	-	-	-	-	-	-	-	Results questionable since inj. plugging occurred. Found Al particles in annulus after 117A
116B			-	1.08	436	739	613	606	546	60	110	170	-	-	-	-	-	-	-	
116C			-	1.07	360	784	624	594	545	49	185	234	-			-	-	-	-	
116D			-	N.G	360	834	685	661	660	61	240	301	-	-		-	-	-	-	
117A			-	0.87	258	844	675	662	605	57	347	404	-	-	-	-	-	-	-	
117B			-	1.27	470	788	625	596	530	66	60	126	-		-	-	-	-	-	
117C			-	1.29	440	750	585	562	500	62	60	122	-		-	-	-	-	-	
118A			-	1.10	375	655	484	470	425	45	50	95				-	-	-	-	
118B		X-65 Al	-	1.48	ATM	302	143	131	106	25	91	116	-	-	-	-	-	-	-	Movies to ATM.
119A		-	AP, 50/50 20μ/55μ (O_2 Fluid)	3.80	496	-	-		-	-	-	-	880	765	701	665	100	169	269	Checkout O_2 fluidization.
120		X-65 Al	AP, 50/50 20μ/55μ (O_2 Fluid)	1.13 Al 2.98 AP	ATM	300	-	127	83	44	68	112	421	236	-	182	54	167	221	Movies to ATM for imp.
125A		X-65 Al	-	1.33	475	790	611	600	542	59	67	126	-	-	-	-	-	-	-	Repeat of 117B, 118A to check effect of ~ 0.004 annulus decrease.
125B	Coax- 900 lb	X-65 Al	-	1.08	361	651	476	465	417	59	56	115	-	-	-	-	-	-	-	

TABLE XI

FIRE TEST DATA SUMMARY (1 of 2)

Test No KE-2	Injector Conf	Propellants Fuel	Propellants Oxidizer	t^* Time Sec	Pc Psia	Total Flow Lb Sec	Mixture Ratio O/F	Thrust Lb Test	Thrust Vac Lb	I_{sp} Vac Lb-Sec/Lb	ηI_{sp}	Char. Veloc c^*, Ft/Sec	ηc^*	Pc Oscillation Amplitude Mean Pc	Pc Oscillation Freq. Hertz	Combustor L*
100	Coaxial 500 LBF	CH_4 Gas Start-Al 5 μ with CH_4 Fluid	AP 55 μ	0.8	328	2.71	1.61	491	--	-	--	-	--	44	100	
				1.8	326	2.47	2.69	506	--	--		-	-	19	100	
101		Same as 100 but 10 Mg		0.8	331	2.74	1.89	518	--	-	--		-	38	110	
				1.8	325	2.87	1.98	510	--	-	--		-	23	90	
102		Same as 100 but 15 Mg		0.8	312	3.15	1.41	535	--	--	--	--	--	50	110	
				1.8	320	3.31	1.37	554	--	--	--	-	--	50	100	
103		Same as 100 but 5 μ Al with 10 Mg		0.8	462	3.91	1.78	491	--	--	--	--	-	47	90	
				1.8	444	2.93	1.66	479	--	--	--	--	-	40	70	
104		Same as 100 but 30 Al	55 μ	0.8	501	3.69	1.36	479	--	--	--	-	--	38	110	
				1.8	494	2.84	1.41	532	588	207	0.93	4620	0.99	10	130	
107			AP 20 μ	0.8	394	2.96	0.83	452	511	173	0.78	3640	0.89	11	80	
				1.8	333	2.96	0.51	411	567	192	--	--	--	5	140	
109		Same as 100 but 3μ Al	AP 20 μ +0.2 SiO_2	0.8	384	3.16	1.27	517	--	--	--	--		45	110	
				1.8	381	3.02	1.17	531	--	--	--	-	--	38	110	
110	Coaxial 500 LBF	Same as 100 but X65 Al	AP 55 μ	0.8	330	2.88	1.03	450	--	--	--	--	--	62	105	
				1.8	340	3.01	0.96	488	544	161	0.78	3940	0.92	8	105	83
121	Coaxial 900 LBF		AP 50/50 55/20 μ O_2 Fluid	0.8	450	4.13	3.30	836	--	--	--	-	--	23	80	83 (1)
				1.8	456	4.38	3.57	835	945	216	0.85	4270	0.895	16	75	
122				0.8	422	4.08	2.71	888	-	--	--	-	--	31	110	
				1.8	464	4.34	2.94	885	995	230	0.90	4670	0.965	18	82	
123				0.8	462	5.31	0.91	923	1033	194	0.86	4060	0.935	17	100	
				1.8	430	4.49	2.14	873	--	--	--	-	--	18	65	
124				0.8	476	5.29	0.89	917	1027	194	0.86	4060	0.96	3	53	
				1.8	434	4.32	2.15	860	--	--	--	--	-	7	70	85
126				0.8	475	5.03	1.0	911	1021	204	0.87	4050	0.93	17	80	105 (2)
				1.8	433	4.35	1.72	861	971	224	0.89	4470	0.95	19	55	
127	Coaxial 900 LBF	Same as 100 but X65 Al	50/50 55/20 μ O_2 Fluid	0.8	478	5.41	.99	925	1035	191	0.84	3900	0.92	10	54	
				1.8	453	4.98	1.15	949	1059	212	0.88	4260	0.95	18	58	105

(1) - 5 Barrel 3.50 Dia.

(2) - 7 Barrel 4.05 Dia.

TABLE XI (2 of 2)

Test No.	FFPFP	FFOP Psia	FFP Psia	ΔP_{Line} FFOP-FFP	ΔP_{Inj} FFP-Pc	ΔP_{Sys} FFOP-Pc	W_{Al} Lb/Sec	OFPFP	OTOP Psia	OFP Psia	ΔP_{Line} OTOP-FFP	ΔP_{Inj} OFP-Pc	ΔP_{Sys} OTOP-Pc	W_{AP} Lb/Sec	A_t in.^{2} Pre/Post	Purpose/Remarks
100	503	505	452	53	124	177	1.01	612	692	560	12	232	271	1.67	1.030/1.125	Reference test to evaluate 5# Al and compare with previous tests
	500	503	475	28	149	177	.80	611	695	561	11	180	221	1.67		
101	508	505	461	44	127	171	0.95	615	693	569	14	235	268	1.79	1.125/1.190	Evaluate effect of 10 percent Mg in 5# Al.
	502	499	462	37	137	174	0.98	614	691	571	23	236	279	1.89		
102	510	505	459	46	137	191	1.31	608	686	555	15	243	288	1.84	1.190/1.236	Evaluate effect of 10 percent Mg in 5# Al
	511	508	459	44	149	183	1.31	608	699	561	15	244	279	1.80		
103	730	725	616	119	145	267	0.90	749	736	686	50	221	271	1.60	0.694/0.845	Evaluate effect of 10 percent Mg in 3# Al
	729	714	598	117	134	269	1.11	748	737	692	45	248	295	1.84		
104	781	771	648	123	147	270	1.14	797	788	718	15	242	287	1.55	0.672/0.825	Repeat test, 3# Al, compare with previous program results
	778	753	628	125	134	259	1.18	797	791	747	11	253	297	1.66		
107	675	670	571	99	177	276	1.62	702	657	619	18	225	263	1.31	0.825/0.875	Evaluate 20# AP with 3# Al AP was bulky, AP injector clogging
	675	667	578	89	245	334	1.96	701	693	611	50	310	360	99		
109	644	639	550	89	166	255	1.48	639	593	534	59	150	209	1.68	0.875/1.05	Evaluate 20# AP-SiO_2 with 3# Al/ flow improved, adverse effect on stability
	643	641	563	78	182	260	1.39	636	587	524	63	143	206	1.63		
110	604	598	515	83	185	268	1.12	589	578	526	52	196	248	1.46	1.05/1.08	Evaluate X65 Al
	603	593	514	79	174	253	1.51	588	580	534	46	191	249	1.47		
121	652	647	571	76	121	197	96	739	664	624	40	174	214	3.17	1.255/1.275	Evaluate thrust scaleup, X65 Al, AP blend with O_2 fluidization.
	651	640	589	51	133	184	96	735	676	630	46	174	217	3.42		
122	704	699	608	91	186	277	1.10	746	669	629	40	207	247	2.98	1.275/1.340	Evaluate effect on mixture ratio
	702	687	624	63	160	223	1.10	735	679	642	37	178	215	3.24		
123	746	738	647	91	135	276	2.78	663	607	577	30	115	145	2.53	1.310/1.153	Evaluate effect of mixture ratio/Al injector plugging
	745	730	666	64	236	300	1.43	660	610	573	37	133	180	3.06		
124	760	752	664	88	188	276	2.80	678	610	577	33	101	134	2.49	1.275/1.400	Repeat of previous test Al injector plugging
	7[illegible]	739	685	54	251	305	1.37	676	608	571	37	137	174	2.95		
126	709	699	626	76	148	224	2.52	681	615	589	26	114	143	2.51	1.275/1.390	Evaluate increased Al loading procedure modified
	707	691	618	73	185	258	1.60	679	612	575	37	142	179	2.75		
127	769	755	664	91	186	277	2.85	684	616	583	33	105	138	2.56	1.275/1.457	Evaluate effect of mixture ratio
	767	742	661	81	208	289	2.32	679	619	587	32	134	166	2.66		

amplitude exceeded ±20 percent of mean Pc, or injector plugging occurred. The initial firing test (No. 100) was with H5 Al/55 micron AP. Fire test combustion pressure oscillation level was much more severe, ± 40-44 percent of mean Pc in amplitude, than that obtained with the smaller particle size H3 Al, ±12 percent of mean Pc in amplitude. The next test (No. 101) was conducted with a blend H5 Al + 10 percent by weight magnesium to enhance combustion. The magnesium powder was spherical and screened, 325 mesh (< 44 micron), by the vendor. Combustion stability was improved to ±23-38 percent of mean Pc but the level was still much more severe than that obtained with H3 Al. The concentration of magnesium was increased to 15 percent by weight for the next test (No. 102) which resulted in increased oscillation amplitude, ±50 percent of mean Pc. Testing with H5 Al powder was then curtailed.

Since it was observed that the 10 percent magnesium concentration resulted in reduced amplitude oscillations, a fire test was then conducted (No. 103) with this magnesium concentration blended with original H3 Al powder. A new nozzle was installed. Operating conditions included higher chamber pressure, and mixture ratio compared to the previous tests. Combustion oscillations of ±40-47 percent of mean Pc resulted which were much more severe than with the neat H3 Al powder. A test was then conducted (No. 104) utilizing neat H3 Al powder with a new nozzle. This test resulted in the smoothest combustion obtained at the time with oscillation amplitude of ±10 percent of mean Pc at a frequency of 130 Hertz.

The results confirmed that the Al powder particle size is the dominant influence on combustion stability. Further, the results indicated that smaller particle size magnesium is needed to improve stability of the H3 Al.

The next tests were concerned with evaulating 20 micron AP with H3 Al as a means of improving combustion stability. Two injector cold flow tests, see Table X, were made. This finer AP powder exhibited greater agglomeration tendency and was more difficult to load than previous powders. The initial flow test was unsatisfactory. New powder was vacuum oven dried and the second flow was satisfactory. A fire test (No. 107) was then conducted, which resulted in oscillation amplitude of ±5-11 percent of mean Pc. The oscillation amplitude was somewhat greater near start and reduced to ±5 percent during the last 0.5 second of operation. A surge in oxidizer feed pressure was indicated on the oscillograph at 1.4 seconds from start and mixture ratio was much lower than intended. Injector plugging of about one third of the AP flow area was observed upon post test inspection.

Since this finer AP resulted in smoother combustion, attention was then directed toward improving its physical character. An anticaking agent, 0.2 percent by weight - fumed SiO_2 (Cab-O-Sil) was blended with the 20 micron AP. Improved physical character was immediately obvious and ease of loading was noted. Cold flow tests were satisfactorily completed prior to conducting a fire test (No. 109) with the AP + SiO_2. Stability was adversely affected by the SiO_2 additive with combustion pressure oscillations of ±38-45 percent of mean Pc. It was postulated that the SiO_2,

whose melting point is about 3000° F, coated the AP particles and inhibited heat up and deflagration processes. This suggested the need for a more volatile additive.

A final test (No. 110) was made with the 500 pound hardware to evaluate the effect of Alcan X-65 Al powder on combustion stability. This powder, of 7.4 micron mass median diameter, was selected as a substitute for the H3, of 6.2 micron mass median diameter, which was no longer available. AP powder of 55 micron nominal diameter was used for this test. Combustion oscillations of ±62 percent of mean Pc occurred which smoothed to ±8 percent during the last 0.3 seconds of operation. A trend of reduced oscillation amplitude with increasing run duration was observed during all tests. However, this last test indicated the largest and most pronounced change of all the tests. Maximum specific impulse performance efficiency of 0.93 was derived from the 500 pound thrust tests.

Based on the results of the 500 pound hardware testing, it was determined to conduct the 900 pound thrust chamber test program with the X-65 Al fluidized with methane and a blend of 20/55 micron AP fluidized with oxygen. The use of oxygen as a fluidizer for AP was selected since it would be reactive and enhance burning of Al. Methane was used with Al for all the previous tests, whereas nitrogen had formerly been used with the AP.

Blends of 55 and 20 micron ammonium perchlorate powder were prepared and qualitatively evaluated for flow character. The purpose of this work was to select a blend of AP containing a large fraction of the fine component to enhance combustion and yet provide satisfactory flow character typical of the coarse particle powder. A 50-50, by weight, mixture was selected and a series of cold flow tests were conducted with the coaxial injector, with center oxidizer vortex and fuel annulus. A total of six oxidizer flows as summarized in Table X, were conducted with AP powder at varying tank pressures. The tests covered a range of flows from 2.54 lb/sec to 3.20 lb/sec. One of the tests was made flowing to atmosphere and was recorded with high speed movies. Review of the movies showed that the flow character of the AP was the best observed compared to all previous cold flows. The injector ΔP at rated flow of 3.15 lb/sec was determined to be approximately 175 psi. The flow calibration data are presented in Figure 8. Also shown are water flow data at equivalent flow rates and discharge pressure of 100 psi for use in calculating orifice discharge coefficients shown below:

Injection Orifice Discharge Coefficients, Coaxial Injector

	Al Annulus	AP Vortex
Water	0.872	0.678
Powder	0.526	0.340

It was noted during cold flow that increased ΔP across the piston was

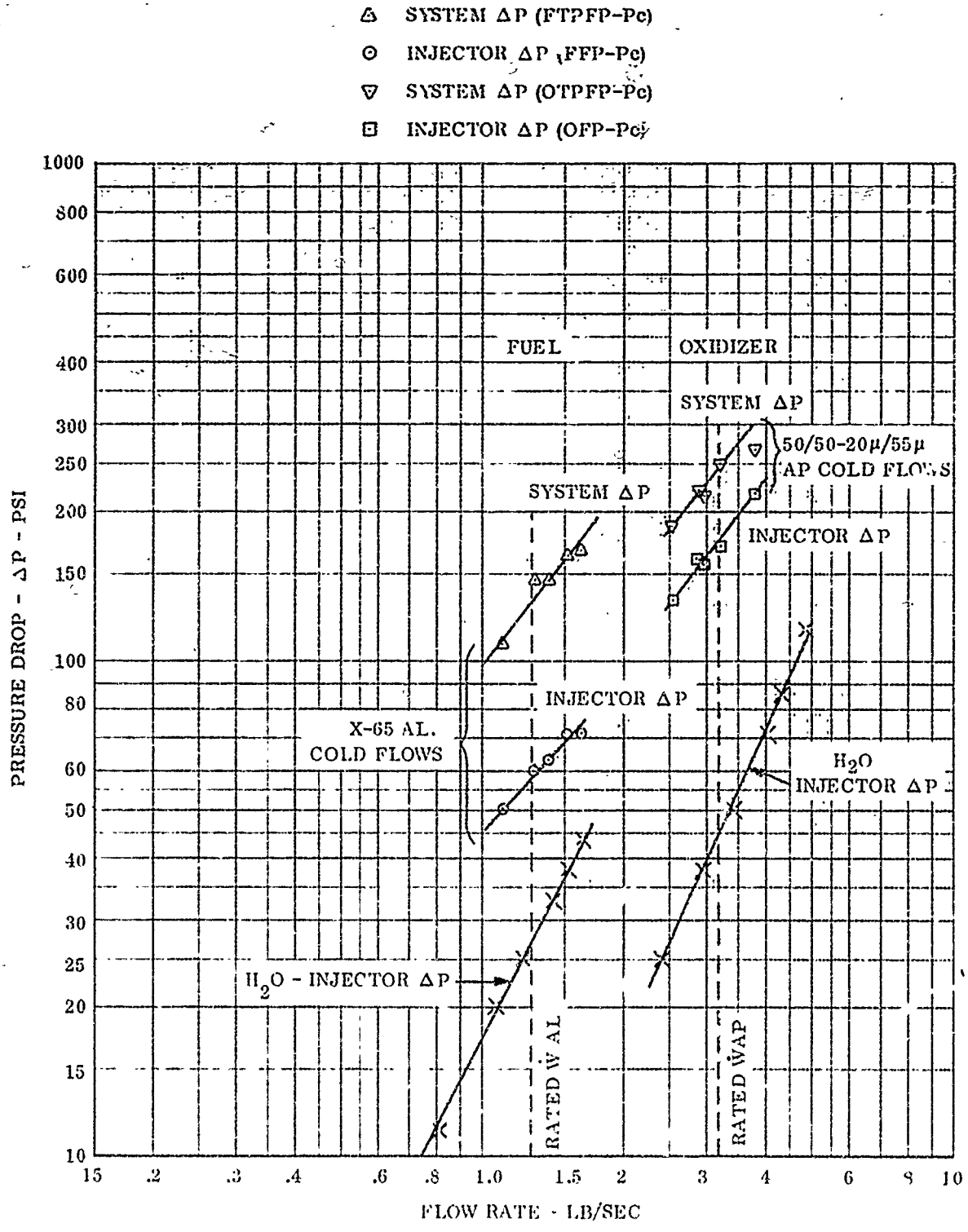

Figure 8. Cold Flow Characteristics of Coaxial Injector

required to maintain piston contact with the fluidized bed during expulsion. For example, at the increased 900 pound thrust flow rates, 180 to 200 psi ΔP was required where formerly at the 500 pound thrust flow rates 100-150 psi ΔP was satisfactory. The increased ΔP was attributed to the greater piston acceleration required for the increased flow rate. Nitrogen was used for fluidization on all tests. Additional cold flow tests were performed to evaluate the O_2 fluidization setup and to record oxidizer/fuel flow impingement.

A total of twelve fuel flows, as summarized in Table X, were conducted through the fuel annulus of the coaxial injector using X-65 aluminum powder. The tests were at varying tank pressures and covered a range of flows from 1.10 to 1.61 lb/sec. Five of the tests were determined to be unsatisfactory due to a progressive buildup of aluminum particles at the entrance to the annulus, causing plugging and excessive ΔP. Two of the tests were made flowing to atmosphere, one of Al alone and one impingement with the AP which were recorded with high speed movies. Review of the movies showed that the flow character of the Al alone and AP/Al together was uniform. The fuel injector ΔP at the rated flow of 1.26 lb/sec was determined to be approximately 60 psi. The fuel flow calibration data can also be seen in Figure 8, with the water flow calibration data.

Photographs of the powder injection stream patterns AP alone, Al alone and AP/Al together can be seen in Figure 9.

As mentioned previously, a pyrotechnic igniter was developed for this program. The required igniter load was scaled up from the 500 pound thrust test program and determined to consist of; a S-67 (DuPont) squib, 4 grams of No. 4895 smokeless powder, and 40 $BKNO_3$ pellets (12.4 grams). A total of six igniter tests were made in the 85 L* chamber to evaluate pressure rise and firing duration. Values of approximately 20-25 psia and 150-200 milliseconds were obtained.

Six fire tests were conducted at the 900 pound thrust level to evaluate the coaxial injector. The operating conditions and test results are summarized in Table XI. Thrust chamber test installation is shown in Figure 10. The objective of the initial test (No. 121) was to establish the effect of thrust level scale-up. This firing was the first to use the 50/50 by weight blend of 55/20 micron ammonium perchlorate powder with oxygen fluidization gas. The test was satisfactory except that the mixture ratio of 3.45 was higher than the planned value of 2.5. Combustion oscillation level was $\pm$ 16-23 percent of mean Pc. Review of the data indicated that the fuel injector pressure drop increased compared to cold flow test results, from 60 to 150 psi at rated flow rate.

The objective of the next three tests (Nos. 122, 123 and 124) was to determine the effect of mixture ratio on operation. Combustion oscillations increased to $\pm$18-34 percent of mean Pc during Test No. 122 which was conducted at a somewhat lower mixture ratio than the initial test. Fuel injector plugging was observed during Test 1CE-123, and several large particles of extruded aluminum were found in the annular orifice approach region, see Figure 11. Since the aluminum powder is

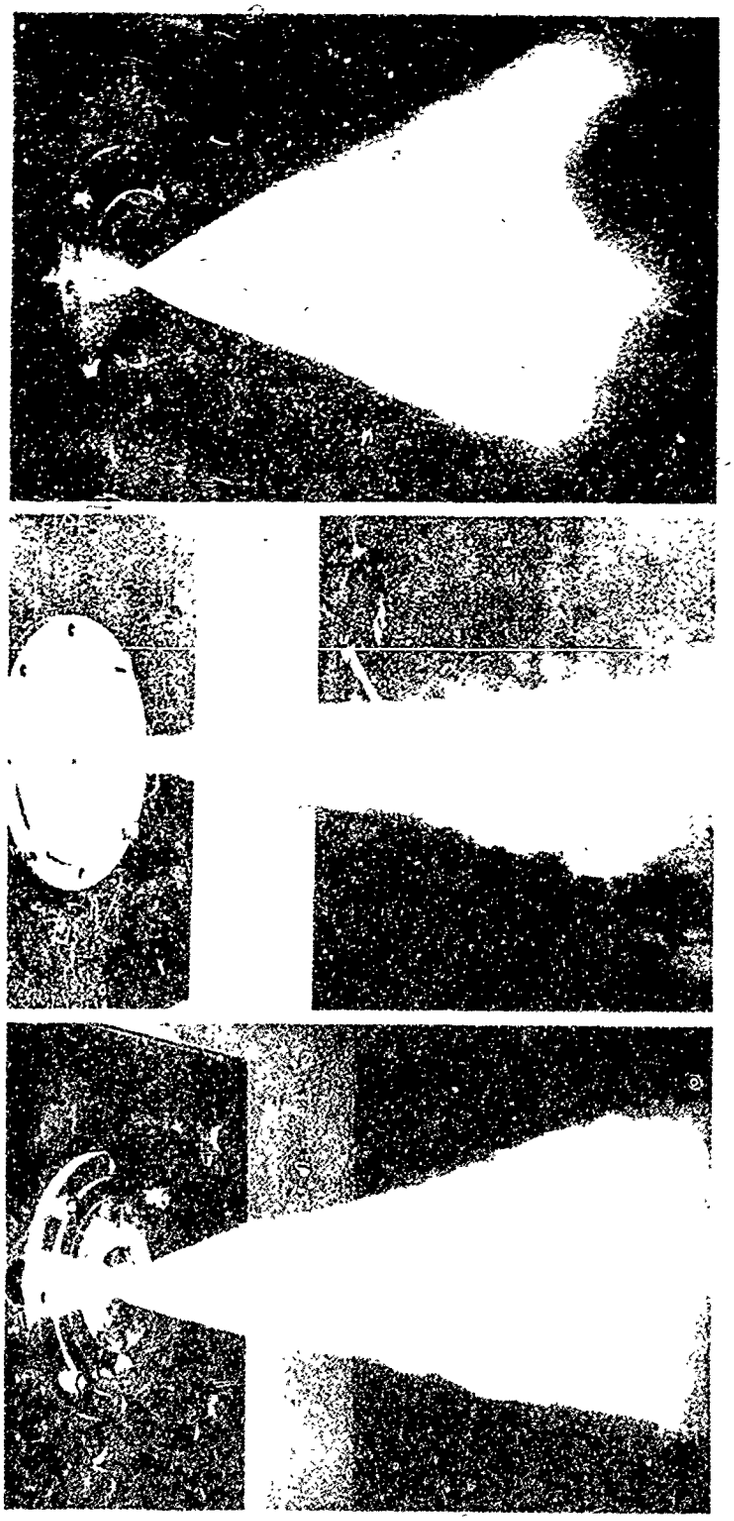

AP

RUN NO. 113D
(NEG. NO. 325630)

AL

RUN NO. 118
(NEG. NO. 325745)

AP/AL

RUN NO. 119
(NEG. NO. 325746)

Figure 3. Powder Cold Flow Views, Coaxial Injector

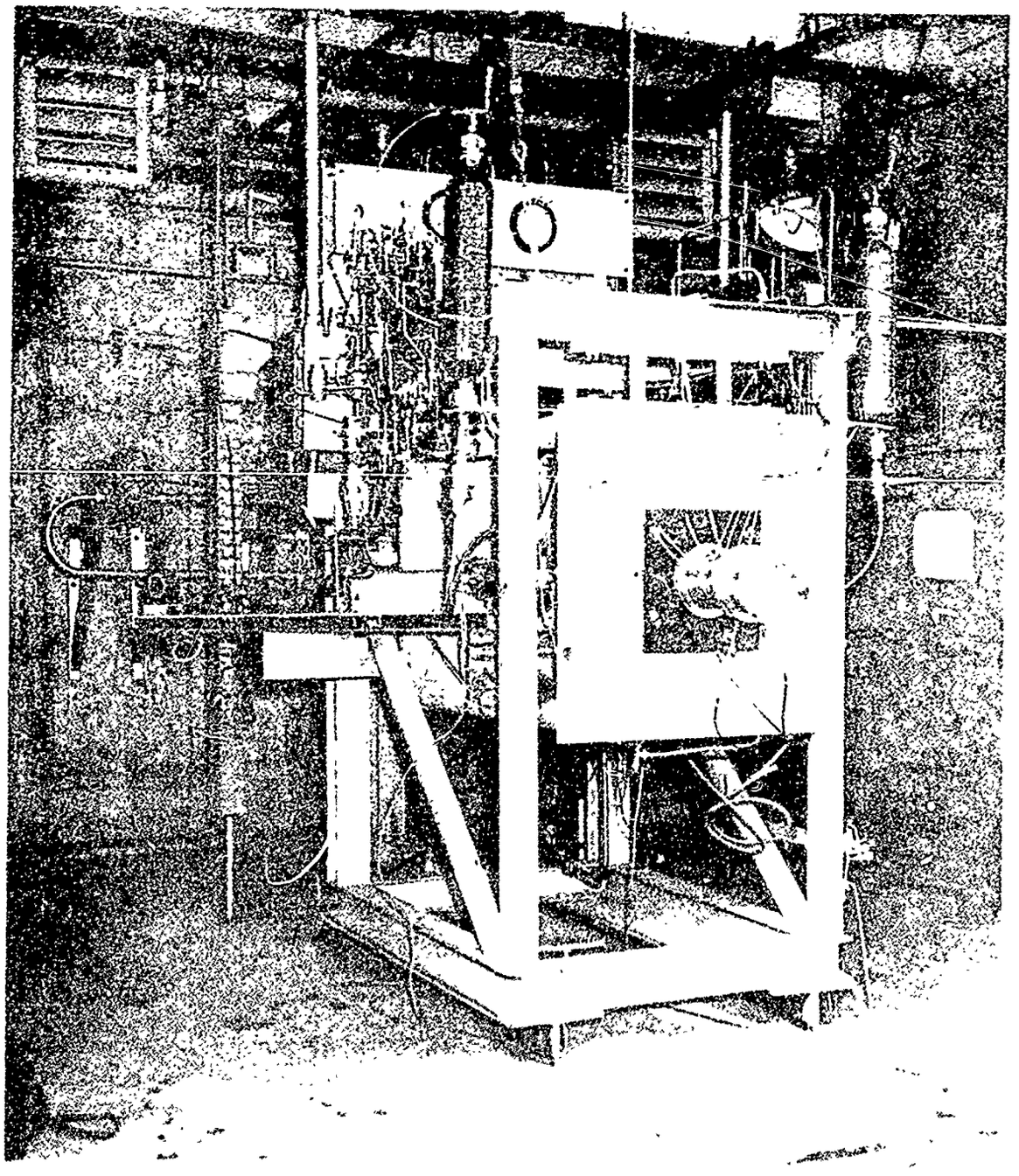

325858

Figure 19. Thrust Chamber Test Installation

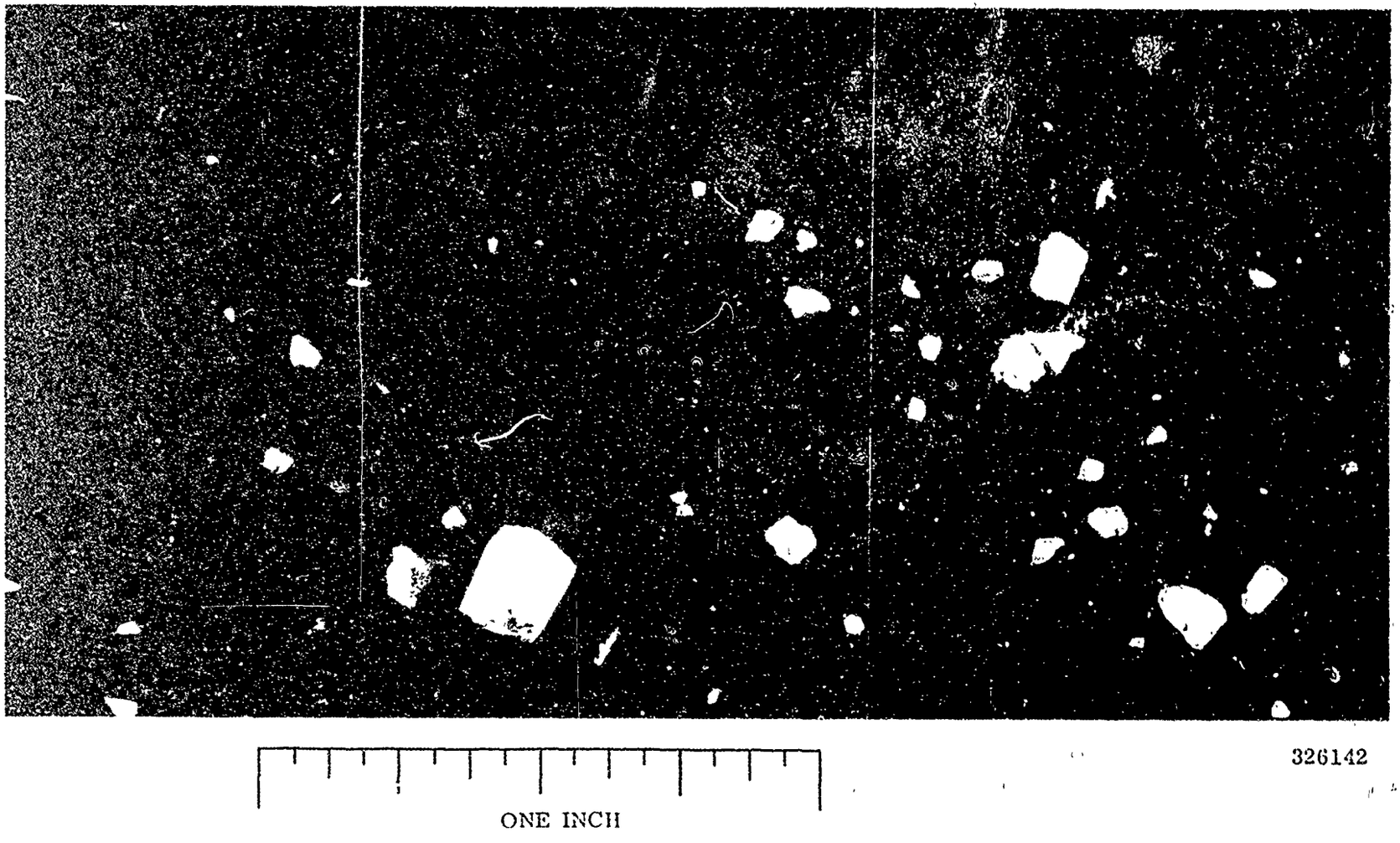

Figure 11. Aluminum Particles From Injector Orifice Approach - Post Test 123

screened prior to loading the extruded aluminum was considered to be formed by mechanical action in the piston fluidization tank or flow control valves. Test 1CE-124 was a repeat of the previous test but fuel injector plugging recurred. Combustion stability level during test number 124, was ±3 percent of mean Pc near start, increased to about ±13 percent at 1.0 seconds and then decreased to ±7 percent at 1.8 seconds. Although fuel injector plugging occurred during the mixture ratio test series some trend in combustor operation was observed. Specific impulse efficiency was highest (0.90) at 2.94 O/F with lower efficiency indicated at higher and lower mixture ratios. Combustion oscillation amplitude was lowest (±3 percent of mean Pc) at mixture ratio of 0.89, and was observed to worsen as mixture ratio was increased to 2.71 (±34 percent of mean Pc). Post test inspection again showed the accumulation of large size aluminum particles in the fuel annulus of the injector. Measurement of the fuel annulus gap also showed a 0.002 to 0.004 inch reduction in the 0.030 inch fuel annulus gap, which accounts for a portion of the injection pressure drop increase.

In order to verify this, two additional X-65 aluminum cold flow tests were conducted to verify injector pressure drop and provide information relative to the plugging problem, utilizing the powder which remained in the tank from Test 124. No plugging occurred and the injector pressure drop was only 5-8 psi higher than the original cold flow data. Cycling of the aluminum load valve was then considered to be causing the formation of large particles and a procedure was instituted which eliminated valve cycling during fill.

Two additional fire tests, 1CE-126 and -127, were made to evaluate the effect of the 105 L* chamber on combustion stability. Run conditions were maintained similar to Test 1CE-124 in order to achieve a similar mixture ratio. No injector plugging occurred on these runs, which substantiated the loading theory. The 105 L* results indicated slightly higher specific impulse efficiency and Pc oscillation amplitude compared to the 65 L* tests.

An oscillograph record of Test 127 is presented in Figure 12. It is shown that oscillations are evident in combustion pressure and fuel and oxidizer feed pressures but the fluidized bed tank outlet pressure traces were smooth. Also, the feed pressure traces are about 180° out of phase with combustion pressure.

Some difficulty was experienced in the test setups to vary mixture ratio for the fire tests. This was due to an increase in Al injector pressure drop compared to cold flow tests as shown in Figure 13. The cause of this pressure drop increase was apparently related to combustion operation since pre and post fire test cold flow characteristics were essentially unchanged.

Maximum specific impulse performance efficiency of 0.090 was derived from the 900 pound thrust tests.

Testing of the 900 pound thrust premix injector was deleted from the test plan. Based on 500 pound thrust tests, it was believed that this injector configuration would not produce results different from those obtained during testing of the coaxial unit.

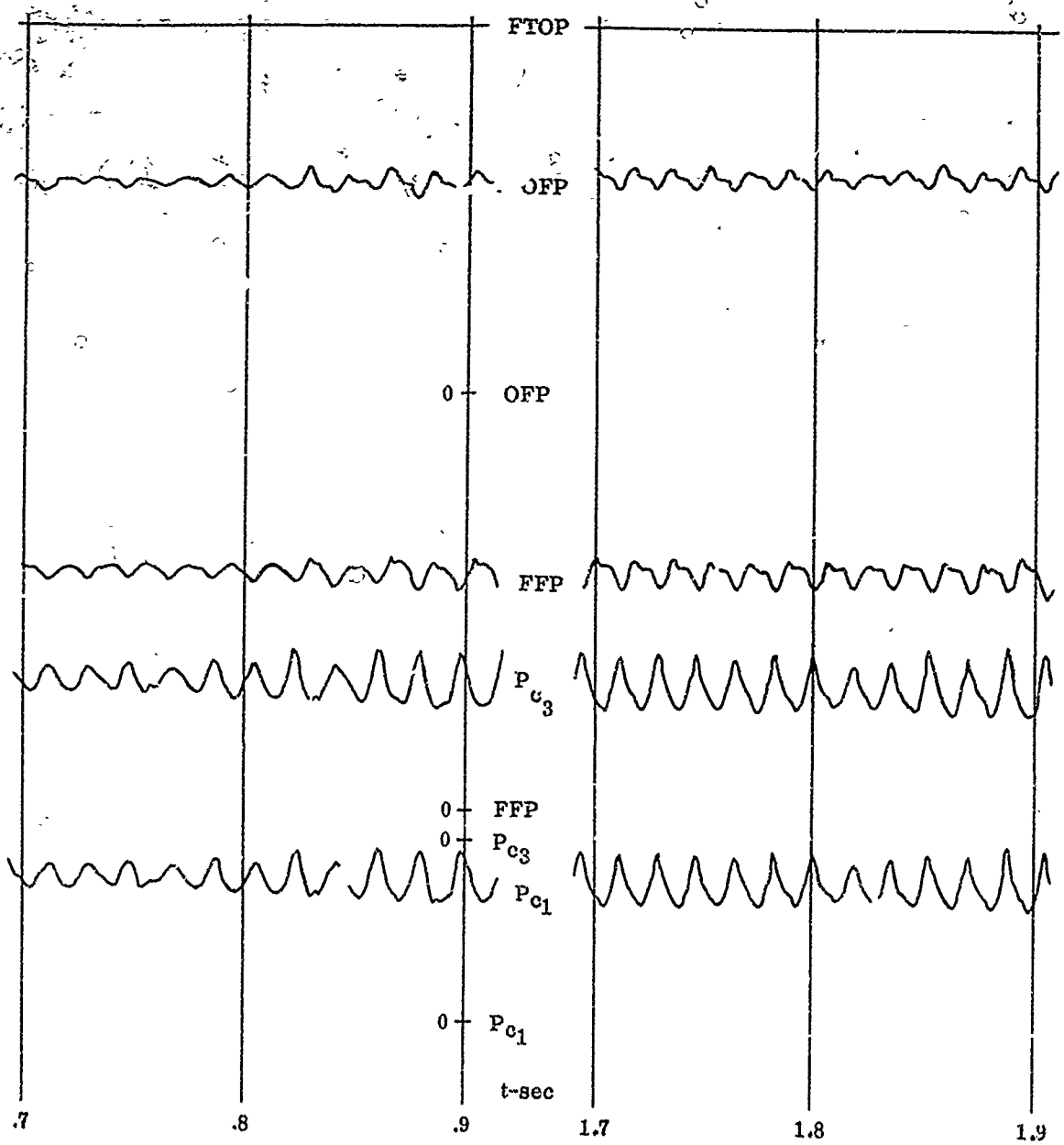

Figure 12. Oscillograph, Test 127

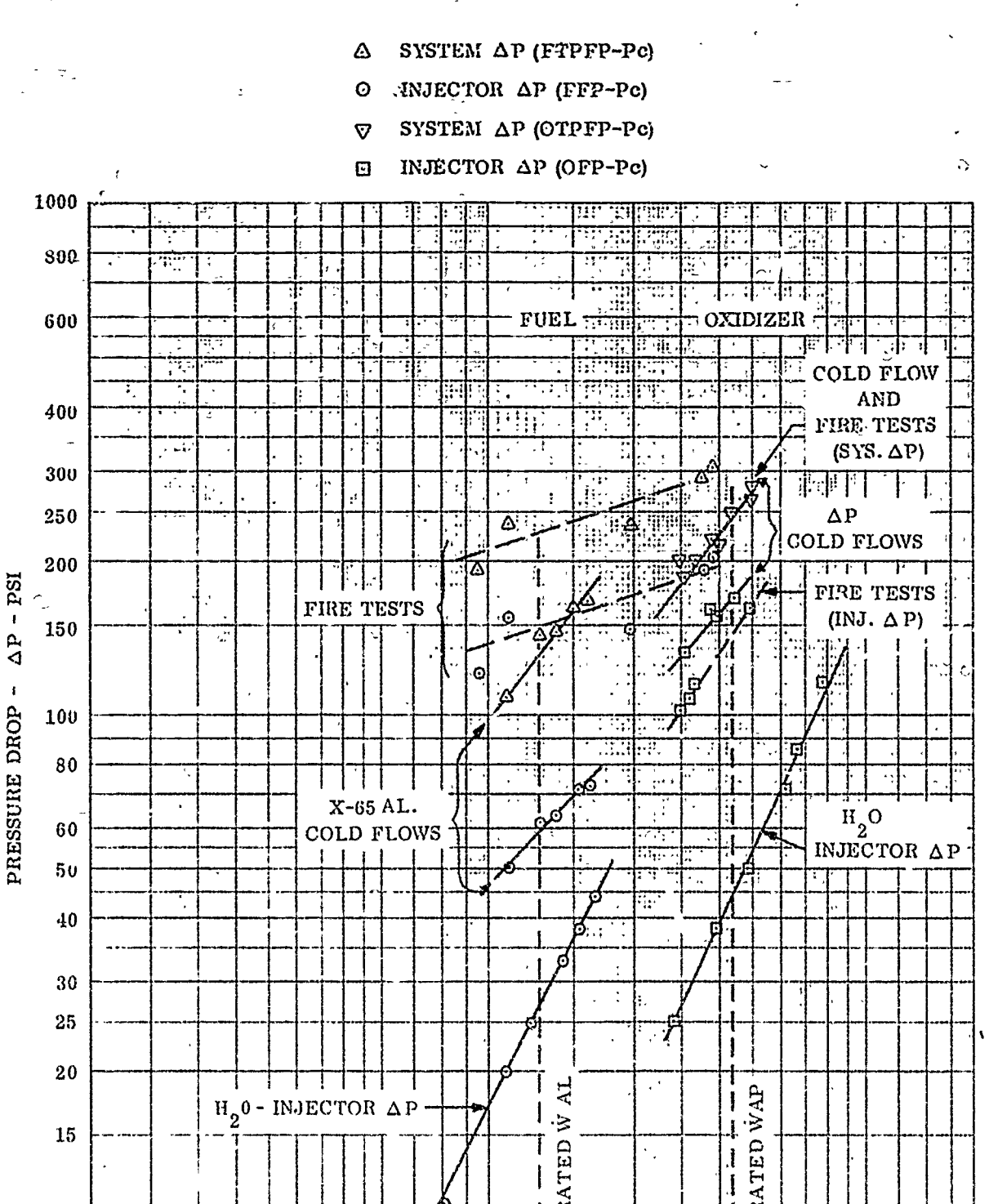

Figure 13. Fire Test and Cold Flow Characteristics of Coaxial Injector

Bed Calibration

Bed calibration was determined during cold flow by measuring the powder efflux. Mass flow rate dW_s/dt was correlated with bed piston displacement (D) using a linear potentiometer. The fire test flow rate could then be derived from bed displacement according to the following equation:

$$\frac{dW_s}{dt} = \bar{K} \frac{dD}{dt} \qquad (1)$$

where $\bar{K}$ is the bed flow constant in terms of mean solids weight expelled per unit displacement of the fluidized bed. Fluidization gas was vented from the receiver; so, only the solids are included in equation (1). Bed calibration data are presented in Table XII. Packing efficiency (defined as the ratio of bed density to particle density) of AP and Al was derived from the cold flow data.

Fluidization gas was measured during expulsion with flowmeters located at the inlet to the bed fluidization port. The total mass flow rate (dW_{gt}/dt) of fluidization gas is that which occupies the propellant interstices at bed pressure and temperature under static conditions (dW_{gs}/dt) plus that which enters during expulsion (dW_{gi}/dt) or stated in equation form as follows:

$$\frac{dW_{gt}}{dt} = \frac{dW_{gs}}{dt} + \frac{dW_{gi}}{dt} \qquad (2)$$

where $W_{gs} = \frac{PV}{RT}(1-x)$

P = bed pressure - lb/sq ft

V = bed volume - cu ft

R = gas constant - ft/°R

T = temperature - °R

x = packing efficiency

Measurements of the fluidization gas flow rates during fire test are presented in Table XIII.

It can be seen that for all tests the flow rate of CH_4 gas into the Al tank was essentially zero during most of the expulsion, with a very small flow indicated near shutdown. AP fluidization flow was indicated throughout expulsion during the 500 pound thrust testing but only during the last second of operation during 900 pound thrust tests. This is probably due to the difference in AP powders used.

TABLE XII

BED CALIBRATION DATA

Measurement	AP		AL
Bed Flow Constant, $\bar{K}$ Lb/In.	0.510	0.533	0.695
Nominal Particle Size, μ	55	55/20	3
Bed Solids Density, Lb/In.^{3}	0.0405	0.0425	0.0553
Particle Density, Lb/In.^{3}	0.0703	0.0703	0.0976
Bed Packing Efficiency	0.58	0.60	0.57

TABLE XIII

FLUIDIZATION GAS FLOW RATES

Test No. 1CE2	Data Time Sec	AP Tank Lb/Sec		AL Tank Lb/Sec	
100	0.8	N_2	0.0130	CH_4	0
	1.8		0.0141		0.0020
101	0.8		- -		0
	1.8		- -		0
102	0.8		0.0107		- -
	1.8		0.0127		- -
103	0.8		0.0221		- -
	1.8		0.0296		- -
104	0.8		0.0086		0
	1.8		0.0106		0
107	0.8		0.0127		0
	1.8		0.0134		0.0021
109	0.8		- -		0
	1.8		- -		0.0014
110	0.8		0.0093		0
	1.8	N_2	0.0095		0.0010
121	0.8	O_2	0		0
	1.8		0.0124		0
122	0.8		0		0
	1.8		0.0285		0.0013
123	0.8		0		0
	1.8		0.0109		0.0011
124	0.8		0		0
	1.8		0.0104		0.0010
126	0.8		0		0
	1.8		0		0
127	0.8		0		0
	1.8	O_2	0.0113	CH_4	0.0014

Skin Temperature Results

Measurements of the graphite liner exterior skin temperatures are presented in Table XIV. The mean temperature for the chamber region can be seen to be about equal to the value predicted, see Table VI. Also, the discrete temperatures indicate a relatively cool zone near the injector. Throat temperatures are much higher than predicted. This probably results from differences between actual and assumed wall thermal diffusivity properties rather than variation in gas temperature or film coefficient. Here the sensitivity of skin temperature to wall properties would be greater in the throat than the chamber region due to the higher heat flux.

Heat transfer loss to the thrust chamber walls would therefore be approximately equal to the predicted value of 135 BTU/lb, which corresponds to the sum of the chamber and throat specific heat rejection values at 2.0 seconds for the -5 and -7 chambers shown in Table VII.

Exhaust Samples Results

Exhaust samples were collected in the apparatus supplied by the Air Force Rocket Propulsion Laboratory during Tests 121, 123, 124 and 127. An insignificant quantity of product was collected during the initial test. A quantity of white product which appeared like a flame sprayed aluminum oxide coating was collected during the other tests. Samples were removed and pulverized for chemical analyses. Composite samples from each test were analyzed according to the procedure of Reference 6. Results indicated less than 1 percent by weight of unreacted aluminum in each of the samples.

3.2 Powder Packing Evaluation

3.2.1 Approach

The plan for conducting the powder packing effort consisted of three principal subtasks:

a. Conduct packing tests on as-received available powders utilizing monosize, bimodal and trimodal particle distributions with premixed, layered, sequenced and continuous blending techniques. (Subsequently to be described.)

b. Select the best distribution and blending techniques, conduct packing tests with shape modified (rounded) particles.

c. Evaluate the effect of anti-friction agents by conducting packing tests on selected blends with silica, boron nitride, glass microballoons and fluoroethane additives.

A survey of AP suppliers resulted in availability of the following particle size powder for the packing evaluation: 7, 20, 50, 80, 200, 400 and 400 micron (rounded).

TABLE XIV

THRUST CHAMBER GRAPHITE SKIN TEMPERATURE MEASUREMENTS - °F
AT 2.0 SEC

Region	Thermocouple Station From Injector In.	Data Time Sec	Test No. 1CE2-					
			121	122	123	124	126	127
Chamber								
	0.9	2.0	593	726	476	418	529	416
	3.25	2.0	1170	1269	874	899	954	818
	5.85	2.0	1160	1273	1146	1056	1147	1100
	8.45	2.0	1094	1205	1107	1057	1071	1105
	MEAN	2.0	1004	1118	901	867	925	860
Throat								
	12.18	2.0	525	580	591	594	646	669

Average of two thermocouple measurements 90° apart at each axial station.

It was desired to classify the AP powders into narrow cut fractions, however, a vendor for handling hazardous materials was not available.

The volume fractions selected in this effort for the bimodal AP systems was based in part on the work of Westman and Hugill (Reference 7). Using round, washed sand and varying the coarse/fine volumetric ratio, a minimum void (maximum packing) obtained was at a volumetric ratio of 70 percent coarse, 30 percent fine. The particle size of the sand was: coarse, 4-6 mesh and fine, 150-200 mesh. McGeary (Reference 8) using spherical metal shot plotted data which showed a maximum theoretical density at about 70 percent coarse/30 percent fine. Alley and Dykes (Reference 9) reported maximum packing at about 68 percent coarse/32 percent fine in a bimodal system consisting of 27 and 180 micron AP.

The trimodal AP system ratios were taken in part from the work of Alley and Dykes. AP powders selected for the trimodal were 7, 55, and 400 microns to provide a minimum diameter ratio of 7 between commercially available sizes. A ratio of 12/50/38 percent was reported to have the highest bulk density for AP sizes similar to those evaluated in this investigation.

3.2.2 Test Procedure

Material Characterization

Characterization included particle size analysis, particle density and photomicrographic examination. Particle size distribution was determined at Micron Data Laboratory Service, Grimsby, Ontario, Canada, using a Micrometrics X-ray Sedimentation Analyzer Sedigraph 5000. The powder sample was dispersed with a selected dispersing agent in a liquid (Sedisperse - C43143) having proper density and viscosity. Particle detection is accomplished by passing a finely collimated beam of X-rays through the settling particles, with the position of the cell being moved continuously so that the detector position changes from bottom to top of the cell as sedimentation progresses. All movement is synchronized to the X-axis of the recorder to indicate directly the particle diameter. Data transformation is accomplished by a built-in digital program computer that moves the cell through the X-ray beam. This X-ray sedimentation technique was utilized for powders of particle size < 100 microns. Screen analysis was used to establish distribution for particle size > 100 microns.

Particle density was also determined at Micron Data Laboratory Service by the following procedure:

a. Weight of pycnometer, empty and dry.

b. Volume of pycnometer, calibrated.

c. Weight of dry sample in pycnometer.

d. Weight of pycnometer filled with sample and liquid (Sedisperse - C43143 or equivalent).

e. Specific gravity of liquid at test temperature.

f. Weight of liquid in pycnometer (d-a-c).

g. Volume of liquid in pycnometer ($\frac{f}{e}$).

h. Volume occupied by sample (b-g).

i. Specific gravity (density) of sample ($\frac{c}{h}$).

Photomicrographic examination was conducted utilizing a Hitachi Scanning Electron Microscope and magnifications from 116X to 1300X were taken of the ammonium perchlorate powders and the ammonium perchlorate powder blends evaluated in this investigation.

Tap Density

Tap density was determined by pouring a given volume (weight) of powder into a graduate cylinder. The graduate was mounted on the Jolting Volumeter base, with the unit set to run for 1250 taps. Three runs of 1250 taps constitute the laboratory base to establish tap density. Volumetric readings are taken after each run.

$$\text{Tap Density (g/cc)} = \frac{\text{Weight of powder (g)}}{\text{Final volumetric reading (cc)}}$$

The tap density apparatus was a J. Engelsmann A.G. Volumeter JEL ST2 illustrated in Figure 14 which complies with German Standard DIN 53194 and Finishing Trades Standardization Committee. A measuring graduate cylinder was mounted on a base coupled to a cam shaft which rotates at 250 ± 15 RPM.

Packing Modes

Various packing methods including premixed, layered, sequential and continuous, were evaluated during the conduct of this effort. All of the laboratory scale packing experiments were conducted with sample size of 50 ml. A description of the procedure associated with each mode is as follows:

Premixed:

Known gravimetric/volumetric quantities of ammonium perchlorate and/or aluminum powder of selected particle sizes were manually transferred to and mixed in laboratory jars. The powders were blended on a Norton Company, Model 753RM, Jar Rolling Mill operating at 140 RPM, for one hour.

Layered:

Increments of the constituent powders were alternately added to the graduate. The coarse constituent was first added, followed by the fine constituent

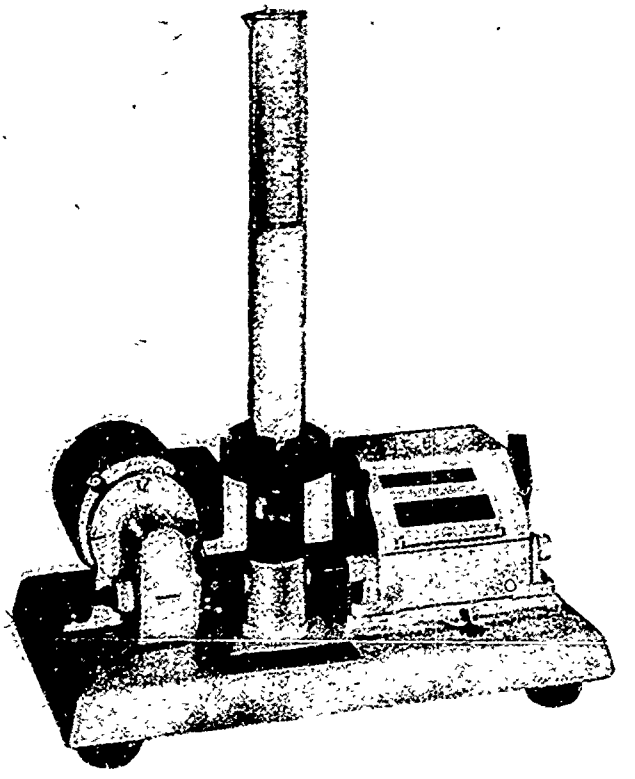

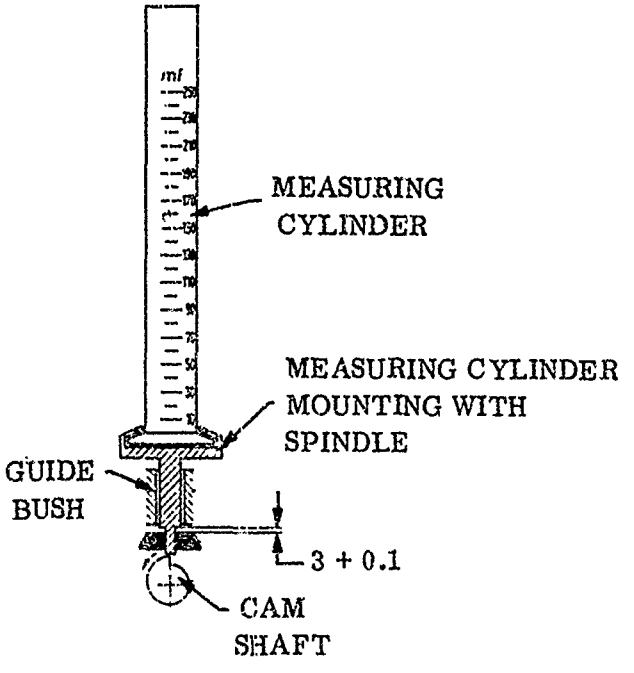

DIAGRAM OF JOLTING VOLUMETER
(DIMENSIONS IN MM)

Figure 14. J. Engelsmann Jolting Volumeter JEL ST2

in turn by the coarse powder followed by the fine powder. This continued until the correct total quantities were added to the vessel, usually ten layers were made.

Sequential:

The entire quantity of the coarse fraction of ammonium perchlorate powder was added to the graduate as one increment. The entire quantity of the fine powder was then added. The graduate was then mounted on the Jolting Volumeter and vibrated with the objective of the fine material penetrating through the voids of the coarse fraction.

Continuous:

Metered quantities in the correct gravimetric/volumetric ratio of the constituent powders are added to the test vessel simultaneously. The powders may be tumbled, vibrated, and/or mixed during the metering cycle. Initial tests were unsatisfactory as the powder flow from the gravity feed system was erratic. Further development effort beyond the scope of this program would be required. Therefore, this mode was approximated in this investigation utilizing a modified layered mode. The size of the layered increments added to the 50 cc graduate was decreased (by one-third and the number increased by a factor of three). Alternate increments of coarse and fine powder was added to the test vessel.

Anti-Friction Agents

Fumed silica, boron nitride and glass microballoons (5 percent by volume) were added to the powder mixture before blending by the premix mode. The fluoroethane liquid was added to the base powder mixtures either before blending or during vibration. The liquid was then evaporated off by placing the mixture in an oven at 175°F for 2 1/2 hours.

Scale-Up

Bimodal AP (20/200 microns) and trimodal AP (7/55/400 microns + SiO_2) blends were scaled up by preparing 11 pound quantities by the premix mode for fire tests. These mixtures were blended for four hours in a Twin Shell Blender.

3.2.3 Test Results

Material Characterization

Particle size distribution results are presented in Table XV which includes the 10, 50 and 90 cumulative weight percent points taken from distribution plots. A typical graph obtained from the X-ray sedimentation technique analysis is shown in Figure 15 which is the characteristic obtained for 20 micron AP.

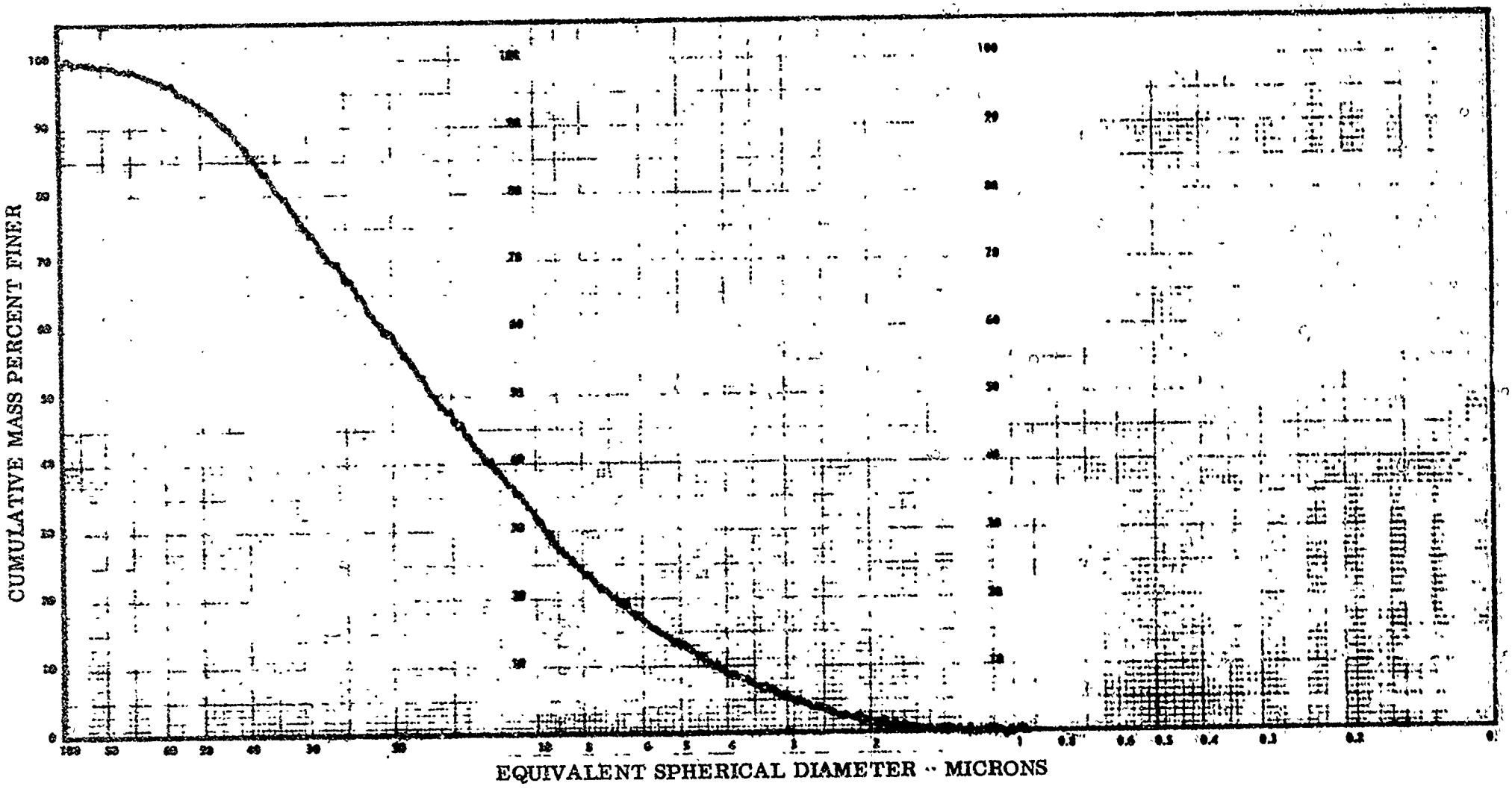

Figure 15. Equivalent Spherical Diameter Versus Cumulative Mass Percent Finer, 20μ Ammonium Perchlorate Powder

TABLE XV

POWDER PARTICLE SIZE DISTRIBUTION

Nominal Size μ	Source	Cumulative Weight % Above Stated Size μ		
		10%	50%	90%
AP				
7	Atlantic Research Co.	14	6	2.7
20	Atlantic Research Co.	44	17	4.2
55	Kerr-McGee	66	38	16
80	Rocketdyne, McGregor	95	72	43
200	Atlantic Research Co.	290	182	105
400	Atlantic Research Co.	490	410	350
400R	Naval Weapons Center	500	420	340
AL				
3	Valley Metallurgical	12	6	3
30	Valley Metallurgical	60	36	20

Particle density measurement results are included in Table XVI. The particle density of the 7 to 200 micron AP powders was 1 94 g/cc, for the 400 micron it was 1.89 g/cc, and for the round 400 micron it was 1.93 g/cc. These values may be compared with the theoretical crystal density of 1.95.

The average particle sizes observed by the Scanning Electron Microscope Micrographs generally agreed with the nominal sizes, although there was a considerable range of size within each sample. The finer particles (7 and 20 microns) showed a high degree of agglomeration making it difficult to define the individual particles. There was no significant difference in shape between the "regular" 400 micron and the "rounded" 400 micron samples, both exhibited a rounded profile. Photomicrographs of each of the base AP powders are presented in Figures 16 through 22.

A significant improvement in the flow character of AP was noted when blended with small quantities of fumed silica. Figure 23 illustrates the structure of a sample with 0.2 percent SiO_2 to improve the fluidity of the powder.

Normally this level of Si would be undetectable by X-ray analysis. However, since Si should be concentrated on the surfaces of the much larger AP particles an attempt was made to detect it. Figure 24 illustrates a reflected electron image and the corresponding Si X ray image. It shows a few scattered Si-rich regions in a nonuniform distribution. Two interpretations are possible. Either (a) the SiO_2 is present uniformly over all the AP particles at a level too small to be detected with the exception of a few heavier concentrations which are detected, or (b) the SiO_2 is located only in a few scattered regions. The improvement in flow of the blends would tend to support the former.

Micrographs of X65 Al powder which was substituted for H3 for fire tests and the H3 are included in Figures 25 and 26.

Tap Density

Powder packing tests were conducted with the base powders, and various combinations of particles including bimodal, trimodal blends and blends with antifriction agents for AP. Tests were also performed with scaled up quantities of AP powders, and AP/Al blends. Powder packing test data are presented in Table XVI and results of each group of experiments are discussed in the following paragraphs.

The tap densities of the seven AP powders selected for this investigation ranged from 0.66 g/cc for the nominal 7 micron particle size to 1.29 g/cc for the nominal 200 micron size. The 400 micron powders had tap densities lower than the 200 micron powder. This apparent anomaly is believed to be due to the spherical shape of the 400 micron powders and the particle size distribution.

The packing efficiencies of the base AP powders ranged from 33.9 percent for the 7 micron to 66.3 percent for the 200 micron particle size.

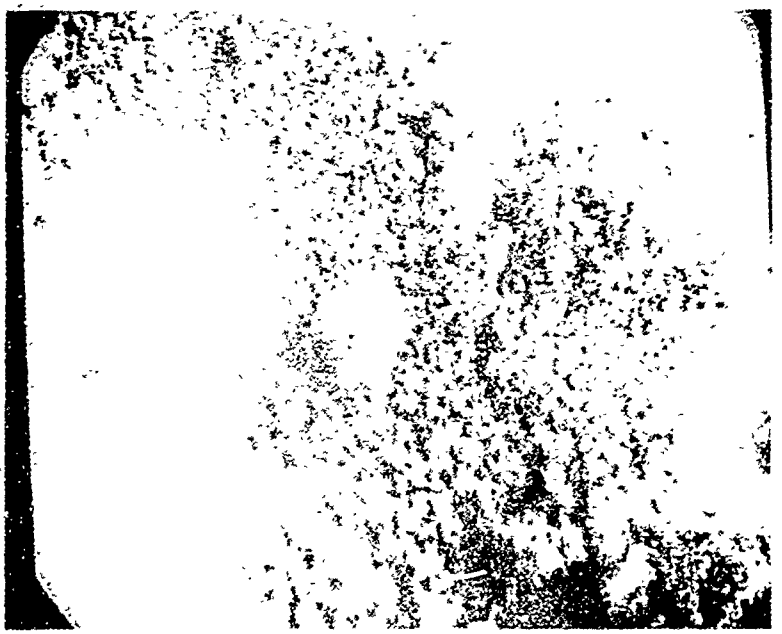

50μ

MAG: 230X

(RES. NO. 574)

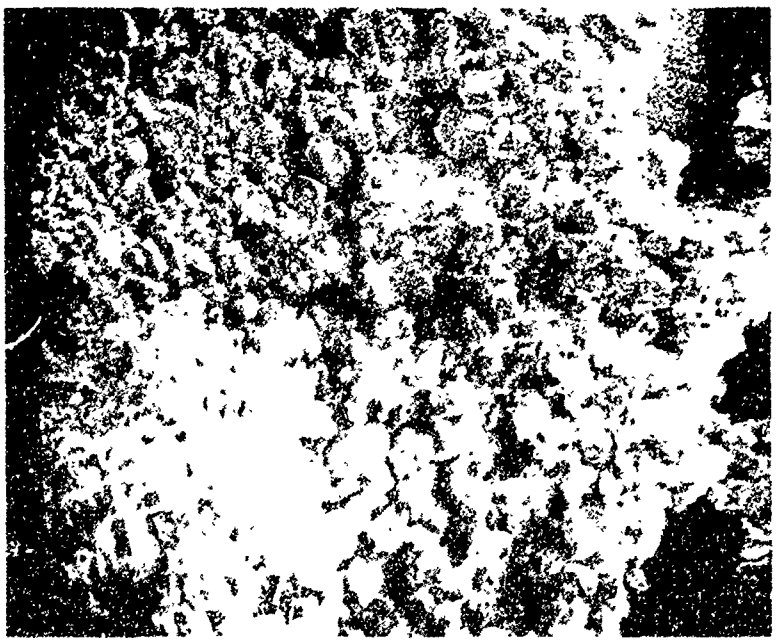

10μ

MAG: 920X

(RES. NO. 573)

Figure 16. SEM Micrographs 7 μ Ammonium Perchlorate Powder

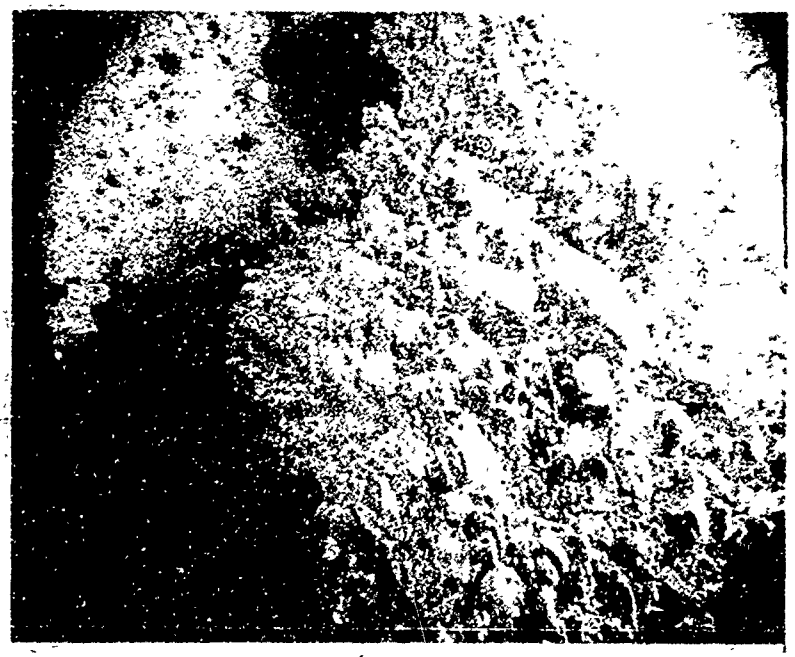

50μ

MAG: 230X

(RES. NO. 576)

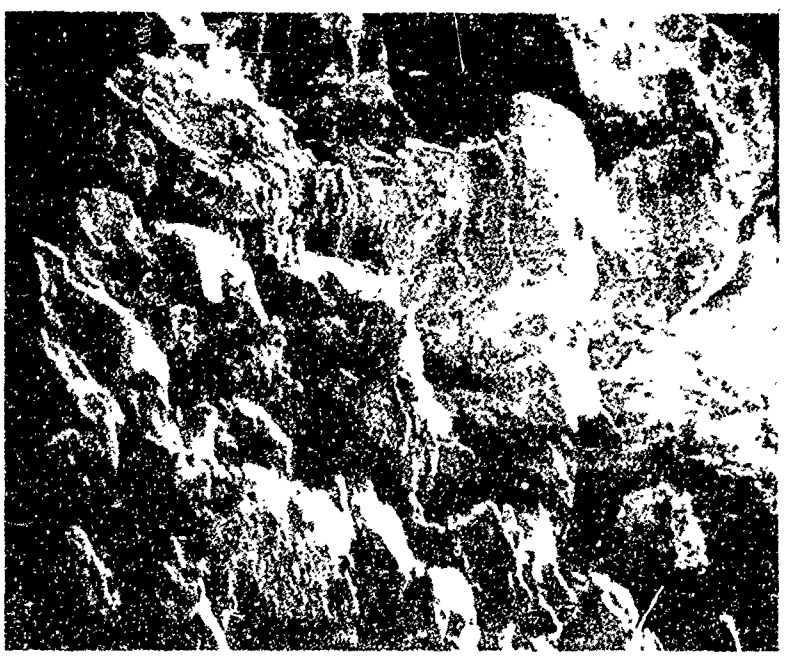

10μ

MAG: 920X

(RES. NO. 575)

Figure 17. SEM Micrographs 20μ Ammonium Perchlorate Powder

50μ

MAG: 230X

(RES. NO. 577)

50μ

MAG: 460X

(RES. NO. 578)

Figure 18. SEM Micrographs 55 μ Ammonium Perchlorate Powder

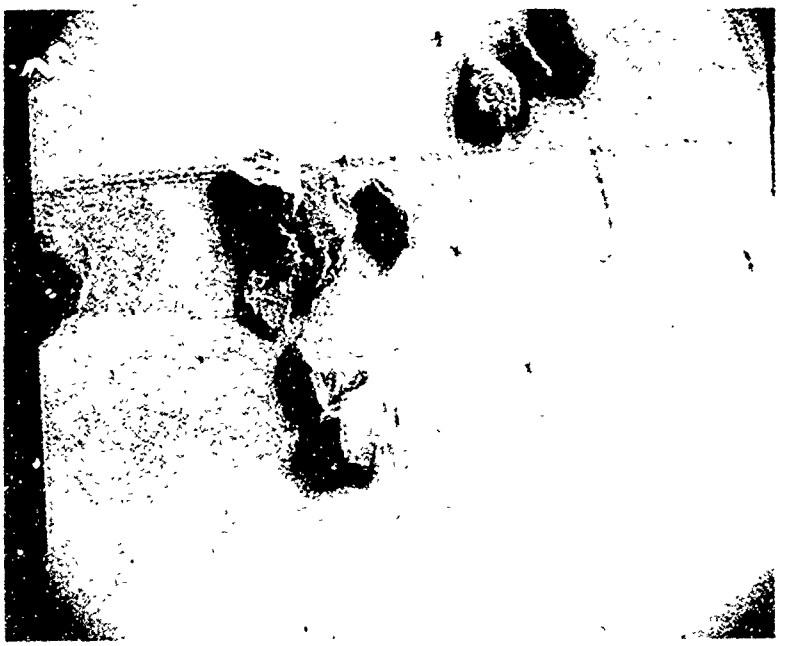

50μ

MAG: 230X

(RES. NO. 579)

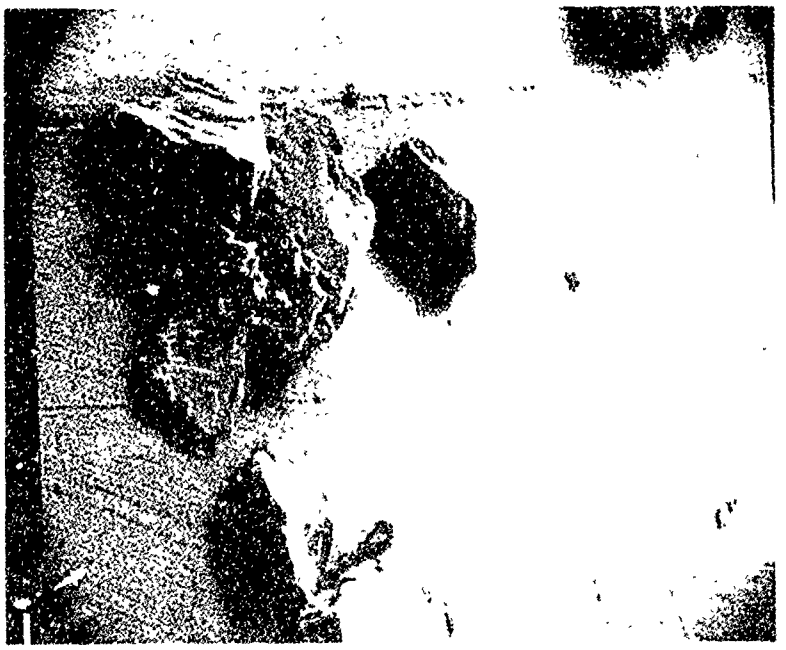

50μ

MAG: 460X

(RES. NO. 580)

Figure 19. SEM Micrographs 80 μ Ammonium Perchlorate Powder

100 μ

MAG: 116X

(RES. NO. 582)

50 μ

MAG: 230X

(RES. NO. 581)

Figure 20. SEM Micrographs 200 μ Ammonium Perchlorate Powder

MAG: 116X

(RES. NO. 583)

100 μ

Figure 21. SEM Micrographs 400 μ Ammonium Perchlorate Powder

MAG: 116X

(RES. NO. 585)

100 μ

Figure 22. SEM Micrographs Round 400 μ Ammonium Perchlorate Powder

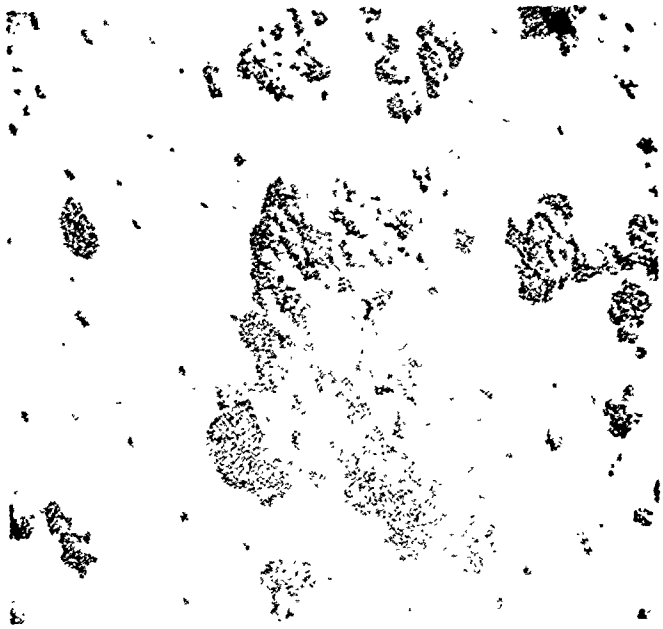

(a)

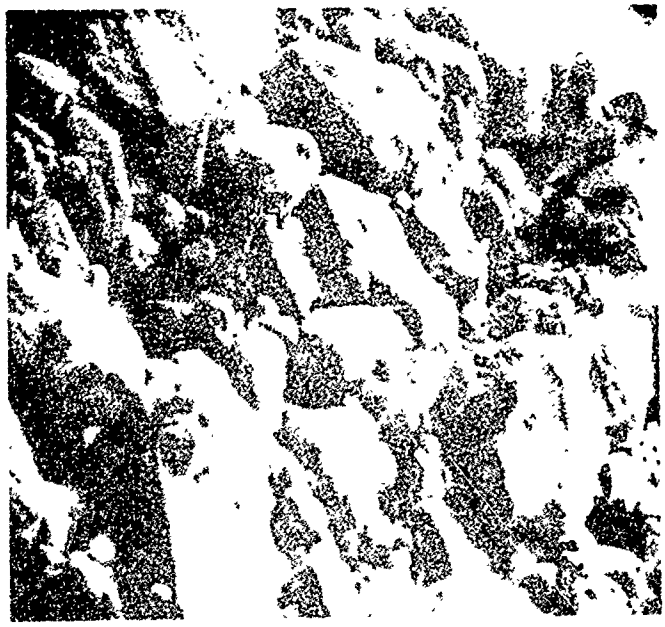

(b)

Figure 23. SE Images of Ammonium Perchlorate Sample No. 4438069C With 0.27 SiO_2 At: (a) Mag: 230X; (b) Mag: 920X

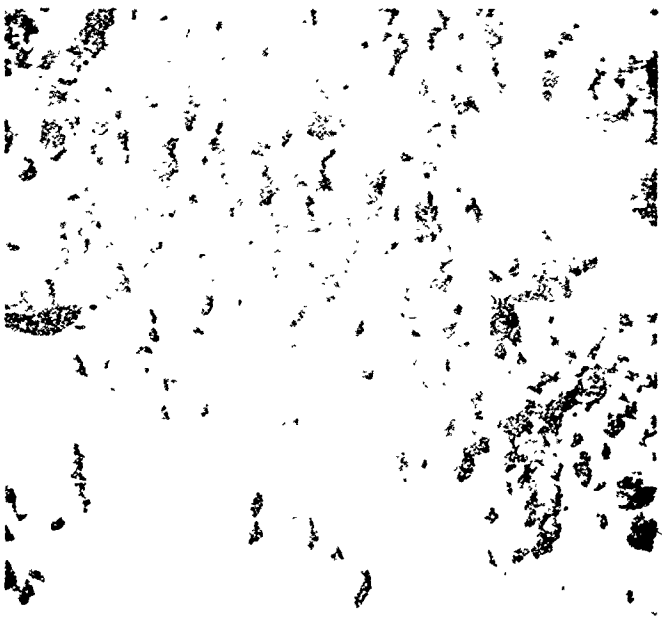

(a)

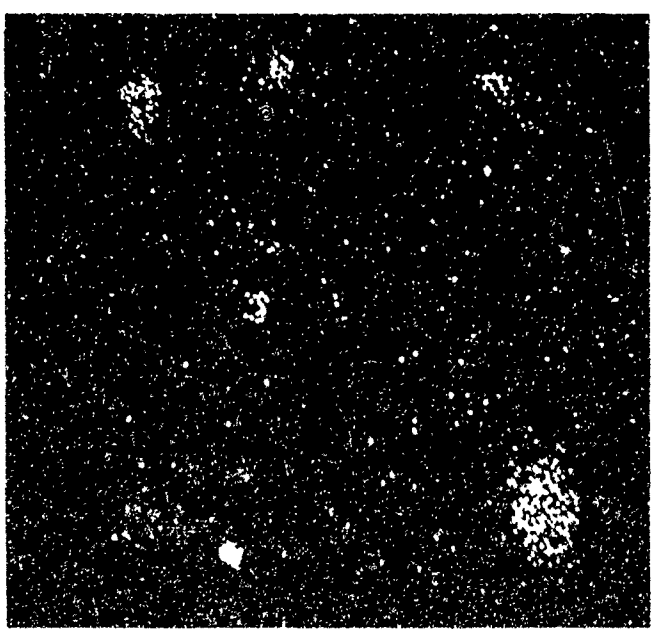

(b)

Figure 24. Ammonium Perchlorate Sample No. 4338069C
(a) Reflected Electron Image
(b) Si X-Ray Image. Mag: 116X

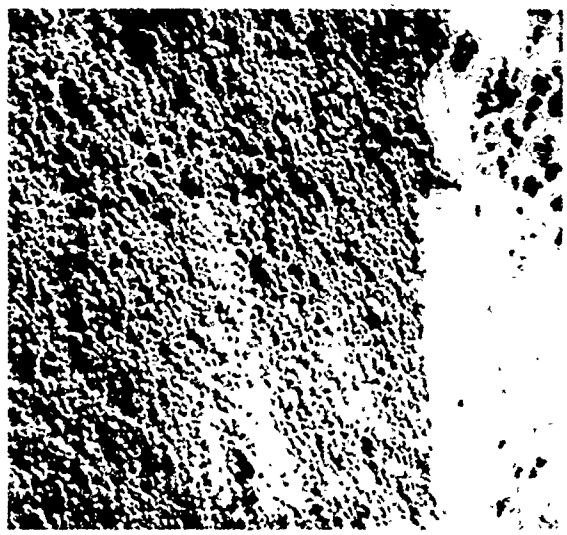

Figure 25. Secondary Electron Images of X65 Aluminum Powder At: (a) Mag: 325X, (b) Mag: 920X, (c) Mag: 1300X

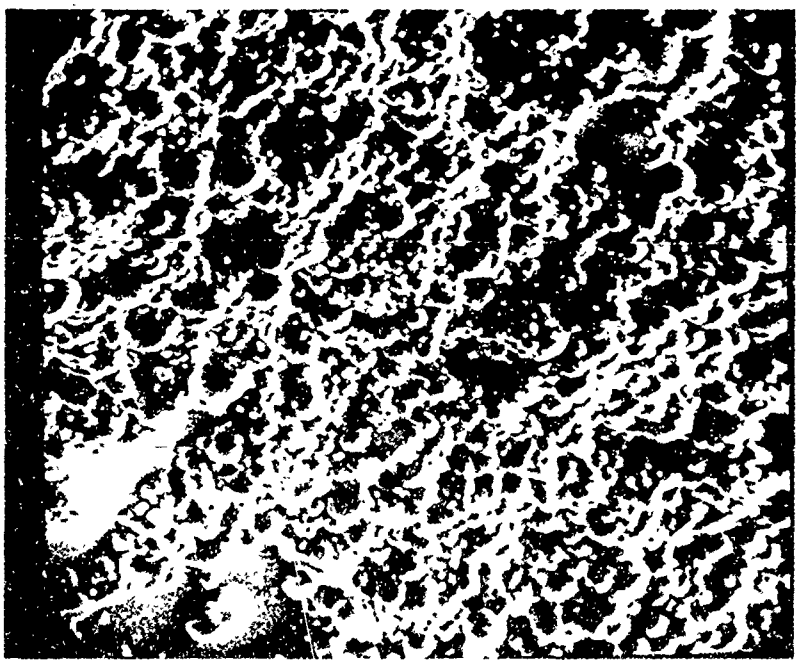

10μ

MAG: 920X (NEG. NO. 142)

Figure 26. SEM Micrographs Valley H3 Spherical Aluminum Powder

TABLE XVI

POWDER PACKING TEST DATA (1 of 3)

Sample	Density g/cc Initial	Tap	Particle Density, g/cc	Packing Efficiency, %
Base Powders [1]				
7 μ AP (6)	0.52	0.66	1.945	33.9
20 μ AP (17)	0.64	0.92	1.943	47.3
55 μ AP (38)	1.05	1.19	1.946	61.1
80 μ AP (72)	1.06	1.20	1.948	61.6
200 μ AP (182)	1.18	1.29	1.944	66.3
400 μ AP (410)	1.12	1.21	1.898	63.7
R400 μ AP (420)	1.18	1.24	1.933	64.1
H3 Al (6)	1.03	1.43	-	-
H30 Al (36)	1.40	1.66	-	-
AP Blends				
Bimodal 20 μ /200 μ (Vol.% 30/70)				
Sequenced	1.01	1.21	1.94	62.3
Layered	1.08	1.22	1.94	62.8
Premixed	1.04	1.35	1.94	69.5
20 μ /400 μ (Vol. % 30/70)				
Sequenced	0.98	1.23	1.90	64.6
Premixed	1.20	1.40	1.90	73.6
Premixed (Repeat Test)	1.14	1.42	1.90	74.7
20 μ /R400 μ (Vol. % 30/70)				
Sequenced	1.03	1.16	1.93	60.1
Premixed	1.13	1.27	1.93	65.8
Premixed (Repeat Test)	1.17	1.29	1.93	66.9
Trimodal (7 μ /55 μ /400 μ)				
a) Vol.%: 12/50/38				
Sequenced	1.00	1.22	1.92	63.5
Layered	0.98	1.32	1.92	68.7
Premixed	1.08	1.41	1.92	73.4

TABLE XVI (2 of 3)

Sample	Density Initial	g/cc Tap	Particle Density, g/cc	Packing Efficiency, %
b) Wt %: 12/50/38				
Sequenced	1.02	1.20	1.92	62.5
Layered	-	1.29	1.92	67.1
Premixed	0.99	1.37	1.92	71.3
Trimodal (7 μ /55 μ /R400μ) Vol. % 12/50/38				
Sequenced	0.96	1.15	1.94	59.2
Premixed	1.04	1.35	1.94	69.5
AP With Antifriction Agents (2)				
Bimodal-Premixed 20 μ /200 μ (Vol. % 30/70)				
a) Fluoroethane	1.04	1.42	1.94	73.1
b) Fumed SiO_2	1.22	1.43	1.94	73.7
c) Boron Nitride	1.05	1.30	1.94	67.1
Trimodal (7 μ /55 μ /400 μ) (Vol. % 12/50/38)				
Layered, fluoroethane	-	1.31	1.92	68.2
Trimodal-Premixed 7 μ /55 μ /400 μ (Vol. % 12/50/38)				
a) Fluoroethane	-	1.44	1.92	75.0
b) Fumed SiO_2	1.14	1.41	1.92	73.4
c) Boron Nitride	1.04	1.33	1.92	69.4
d) Microballoons	1.06	1.34	1.92	69.8
Bimodal AP-Round Shape, Premixed				
a) 20 μ + fumed SiO_2	0.70	1.07	1.94	55.2
b) (20 μ + fumed SiO_2 R400 Vol. %: 30/70	1.24	1.41	1.93	73.0

TABLE XVI (3 of 3)

Sample	Density g/cc Initial	Tap	Particle Density, g/cc	Packing Efficiency, %
c) (20 μ + SiO_2) R400 Conditioned with Fluoroethane	-	1.48	1.93	76.7
AP/AL Blends - Premixed				
200 μ AP/H3, H30 Al (Vol. %: 30/70) O/F = 2.5	1.35	1.50	2.12	70.7
80 μ, 400 μ (Wt %: 50/50)/H3 Al O/F = 2.0	1.23	1.62	2.15	75.3
Scale Up, AP				
Bimodal 20 μ /200 μ - (30/70 % by Vol.)	1.05	1.42	1.94	73.0
Trimodal 7 μ /55 μ /400 μ (12/50/38 % by Vol., + 0.2% fumed SiO_2)	1.22	1.47	1.92	76.5

NOTES: (1) Mass median diameter in microns is given in parenthesis.

(2) Antifriction Agents

Boron Nitride: Atomergic Chemetals Co., Lot C4366, BN - 99 + % (10 μ)

Fumed Silica: Cabot Corp., Cab-O-Sil (SiO_2), Grade EH-5, 0.007 μ, 2.3 lb/ft^3.

Microballons: 3M Co., Hollow Glass Spheres, Lot P-6546B (20-80 μ Range)

Fluoroethane: Bell BMS ST1002-947009, F113, Grade 2 (Ucon 113-LR2), Trichlorotrifluoroethane.

The tap density of a bimodal AP powder mixture with a nominal diameter ratio of 10:1 (200/20 micron) packed by the premix mode was 1.35 g/cc, layered mode 1.22 g/cc, sequential mode 1.21 g/cc, and simulated continuous mode 1.32 g/cc. Packing efficiency ranged from 69.5 percent for the premix mode to 62.3 percent for the sequential mode.

Tap density of a bimodal AP mixture with a nominal diameter ratio of 20:1 (400/20 micron) packed by the premix mode was 1.40 g/cc, and by the sequential mode 1.23 g/cc. Packing efficiency values were 73.6 percent and 64.6 percent, respectively.

Tap density of a trimodal AP mixture (7/55/400 micron) packed by the premix mode was 1.41 g/cc, layered mode 1.32 g/cc, and sequential mode 1.20 g/cc. Corresponding packing efficiencies ranged from 73.4 percent to 62.5 percent. Slight increases in tap density were obtained with the trimodal (7/55/R400 micron) blend.

It was established from the preceding tests that the premix mode produced the highest density, therefore this method was selected and used during subsequent tests.

Treating AP powders with fluoroethane improved the tap density of both the bimodal (20/200 micron) and trimodal (7/55/400 micron) systems. Similar improvements were noted by adding fumed silica to the AP powders. A decrease in density was noted when either boron nitride or hollow glass spheres (microballoons) were added. Characteristics of the anti-friction agents are included in Table XVI.

A packing efficiency of 70.7 percent was obtained by mixing 200 micron AP powder with a blend 30/70 percent by volume of Valley H3/H30 spherical aluminum powder at an O/F ratio of 2.5. An efficiency of 75.3 percent was obtained by mixing a blend of 80/400 micron AP, 1:1 by weight, with H3 spherical aluminum powder at an O/F ratio of 2.0.

It was considered important for propulsion system application to establish if the laboratory processes could be scaled-up without loss in packing efficiency. Therefore, scale-up tests were conducted by preparing 11 pound batches of the bimodal (20/200 micron) and the trimodal (7/55/400 micron + SiO_2). Tap densities of samples of the scaled-up blends showed an increase in packing efficiency of about 3 percent compared to the laboratory size (50 cc) tests.

3.3 Analysis of Experimental Results

Review and analysis of the test results was performed in an effort to correlate data. Due to the exploratory nature of this initial feasibility investigation and the occurrence of combustion instability, a systematic approach was precluded. Emphasis was directed toward diagnosing and eliminating combustion instability. However, the trend of test variables was established. For example, the trend of smoother combustion with reduced particle size of the powder was established.

A systematic test plan was accomplished in the performance of Task II, Powder Packing. Discussion of the results of both tasks is included in the following subsections.

3.3.1 Combustion and Feed System Evaluation

Low frequency combustion instability was encountered during fire tests of the previous program. Reference 1. It was determined that Al powder was the dominant factor affecting combustion stability. Use of smaller particle size Al and reactive fluidizing gas (methane) for Al improved combustion stability. It was postulated that feed system coupled instability forced by the heat-up and combustion lag of Al occurred. However, since the Al which produced the smoothest combustion was no longer manufactured initial contractual fire testing was conducted utilizing existing 500 pound thrust hardware for the purpose of selecting Al and AP powders for 900 pound thrust investigation.

The instability persisted during the contractual program and the test results support the Al heat up and burning hypothesis for combustion oscillations. Three different Al powders were evaluated and the trend of reduced oscillation amplitude with decreased particle size was observed. Additionally, the 5 micron Al exhibited a screening anomaly which suggested particle surface differences which could have affected combustion.

Addition of 10 percent, by weight, 44 micron spherical magnesium powder to Al resulted in reduced oscillation amplitude with 5 micron Al but caused more severe oscillations when blended with 3 micron Al. These results indicate that smaller particle size magnesium is needed to improve stability of 3 micron Al.

Variations in AP powder also resulted in reduced combustion oscillation amplitude with smaller particle sizes. However, the 20 micron AP exhibited a marked tendency to bulk and agglomerate and injector plugging occurred during fire test. Addition of SiO_2 (Cab-O-Sil) improved the physical character of the AP but combustion oscillation amplitude was adversely affected. It was postulated that the SiO_2 coated the AP and inhibited its deflagration processes. This suggests the need for a more volatile anti-caking additive which would gasify or decompose upon entry into the combustion chamber.

A trend of reduced oscillation amplitude with run duration was observed in nearly all tests. Since a heat sink type combustion chamber was utilized in which graphite gas side wall temperatures of about 2000°F were reached in a 2.0 second duration firing it would be expected that heat up and burning of Al would be enhanced with time. This could be attributed to reduced heat loss from the combustion gases and/or radiative heating effect of the wall on Al particles.

Although fuel injector plugging occurred during the mixture ratio test series some trends in combustor operation were observed. Combustion oscillation amplitude was lowest (±3 percent of mean Pc) at mixture ratio of 2.89 and increased (±34 percent of mean Pc) as mixture ratio was increased to 2.71.

Increasing the combustion chamber L* from 65 to 105 inches L* resulted in slightly increased oscillation amplitude.

Based on the results derived from this and previous programs, it is indicated that faster heat up and burning of the Al powder is needed to achieve smooth combustion. The faster heat up may be accomplished utilizing reverse flow or stage combustion injection. With the reverse flow configuration the Al powder would be injected from the nozzle end of the thrust chamber and directed, counter flow, toward the opposite end of the chamber where the AP injector is located. In the staged combustion injector the AP would be decomposed in a preburner which exits into the main combustor where the Al is introduced. With development of suitable injectors, it is expected that smooth combustion would be achieved utilizing the larger particle size H30/H3 Al and R400/20 micron AP blends which provided the greatest packing densities.

The change in Al powder injection pressure drop characteristic between cold flow and fire test is not understood. Additional experimental effort is required if fluidized Al powder rocket technology programs are continued.

Another potential problem associated with Al powder is the formation of large granules due to mechanical action which occurs during valve on-off cycling.

This problem could possibly be alleviated by utilizing hardened Al powder.

3.3.2 Powder Packing

The packing of fine powders of necessity involves vast assemblages of particles which are dealt with en masse and therefore statistically. These assemblages form configurations which fall between limits described as random loose or random dense packing. Regular geometric packings are improbable in the extreme.

Random close packings result from random loose packings by the elimination of excess voidage which migrates to the exterior of the mass. This excess voidage is created by substructures sustained by interparticle friction and cohesion. Since random close packing represents a minimum energy state, the internal substructures are unstable and can be made to collapse.

The technique of particle packing to obtain high packing efficiency comprises filling the voidage formed by the nesting of larger particles with smaller particles of such size and proportion as to fit the intersticial spaces.

The deterents to high packing efficiency in assemblages of fine particles are interparticle friction, cohesion and improper sizing. Certain particle characteristics and size distribution relations are known to facilitate the attainment of high packing efficiency. Among these are:

1. A narrow size distribution within the particle fractions.

2. A large difference in the mean-diameter of the fractions.

3. Rounded particle shape.

4. The surface condition.

The first two factors determine the void filling capacity of the aggregate, while the latter two affect interparticle friction and cohesion. The collapse of substructures within the aggregate is supplied by a combination of gravitational, inertial, and physical forces where the inertial and physical force requirement becomes greater as the size of the particles become smaller. Inertial forces are usually supplied by vibrating or jogging machinery. While surface tension and fluid dynamic drag are the type of physical forces applied to bring about the collapse of the substructures and the migration of voidage to the exterior of the particle assemblages.

Almost everyone who has experimented with packings has poured equal spheres into a container and applied tapping. Extrapolated values for the limiting packing densities are found to be 59 percent for random loose packing and 63 percent for random dense packing. When equal spheres, each having different diameters are mixed, higher packing densities are possible. By choosing the proper quantity and size of sphere making up the components of the mixture, the intersticial spaces are filled and the packing efficiency increases. Under idcal conditions, the calculated density limit of a two component mixture is 82 percent. The proper size relation between the components, expressed as the radius ratio, should be at least 7. In other words, the diameter of the larger particle should be at least 7 times larger than the smaller particle. The limiting voidage volume is simply (1 - packing density).

Just as regular geometric packings are improbable in the extreme so too is the existence of equal spheres or discrete monosize distributions. The greater the spread in the distribution, the more the densities will decrease from the limiting densities stated above. Other factors which detract from attainment of ideal density values are; particle surface irregularities, and interparticle cohesion.

The above factors and relationships have been demonstrated with a number of practical systems, most particularly aluminum metal powder which constituted the fuel in the Powder Rocket Propulsion Evaluation Program. ' able XVII summarizes the results of experiments with fine aluminum powder, Reference 2.

The packing of plain powder, 30 microns and greater in size, approaches that of the limiting value R.D.P. The relatively small difference is attributed to the distribution spread. However, when the particle size is very small (3 microns), surface forces begin to predominate and prevent the collapse of substructures within the mass.

Application of those factors which overcome the surface forces have more influence on the very small particles than on the larger. As the table shows, increas-

TABLE XVII

AL POWDER PACKING SUMMARY

Condition	Packing Density (%)	Remarks
R.L.P.* (limit, value)	59	Ref. (1)
R.D.P.** (limit, value)	63	Ref. (1)
B.R.M.*** (limit, value)	82	Ref. (2)
T.R.M.****	94	
30 μ irregular shape	61	as received
3 μ irregular shape	43	as received
60 μ spherical shape	59	as received
30 μ spherical shape	61	as received
3 μ spherical shape	53	as received
60 μ spherical shape	60	classified
30 μ spherical shape	61	classified
3 μ spherical shape	54	classified
60 μ spherical shape	60	dried
30 μ spherical shape	60	dried
3 μ spherical shape	52	dried
60 μ spherical shape	68	isopropanol treated
30 μ/3 μ irregular shape	62	as received
30 μ/3 μ spherical shape	66	as received
30 μ/3 μ spherical shape	71	classified
30 μ/3 μ spherical shape	77	isopropanol treated

* Random loose packing.

** Random dense packing.

*** Binary random mixture, radius ratio approaches infinity.

**** Ternary random mixture, radius ratio approaches infinity.

ing sphericity, presence of lubrication (moisture), and surface treatment, all promote higher packing densities in the small particle mass.

It is also evident from the table that the application of the factors described improves the density of binary mixtures. The difference in density between the highest attainable binary mixture (77 percent) and the B.R.M. limit (82 percent) is believed once again to be due primarily to distribution spread.

Similarily the effect of these factors and relationships were extended to AP powder packing as demonstrated by the test results summary presented in Table XVIII.

TABLE XVIII

AP POWDER PACKING SUMMARY

Condition	Packing Efficiency - %	Remarks
7 μ	34	
20 μ	47	
55 μ	61	
80 μ	62	
200 μ	66	
400 μ	64	
R400 μ	64	
20/200 μ	70	
20/400 μ	74	
20/R400 μ	67	
7/55/400 μ	73	
20/200 μ	73	Fluoroethane Treated
20/200 μ + SiO_2	74	
7/55/400 μ	75	Fluoroethane Treated
7/55/400 μ + SiO_2	73	
20/R400 μ + SiO_2	77	Fluoroethane Treated
7/55/400 μ + SiO_2	77	Scaled-Up

4.0 REFERENCES

1. Powder Rocket Feasibility Evaluation, H. J. Lofus, L. N. Montanino, R. C. Bryndle, presented at AIAA 8th Joint Propulsion Specialists Conference, New Orleans, La., December 1972.

2. Development of Packing Techniques to Maximize Density of Aluminum Powders, Bell Aerospace Co., BLR 71-IOM, December 1971.

3. Eckert, E. R. G., and Drake, Robert M., Jr., "Heat and Mass Transfer", McGraw-Hill Co., 1950.

4. Schacht, Ralph L., Quentmeyer, Richard J., and Jones, William I., "Experim Investigation of Hot-Gas Side Heat Transfer Rates for a Hydrogen gen Rocket", NASA TND-2832, 1965.

5. Hatch, J. E., Schacht, R. L., Albers, L. U. and Saper, P. G., "Graphical Presentation of Difference Solutions for Transient Radial Heat Conduction in Hollow Cylinders With Heat Transfer at the Inner Radius and Finite Slabs With Heat Transfer at the Boundary", NASA TR R-56, 1960.

6. Bell Aerospace Co., LTP 6094

7. AER Westman, H. R. Hugill: The Packing of Particles, Ontario Research Foundation, Toronto, Canada, June 1930.

8. R. K. McGeary: Mechanical Packing of Spherical Particles, J. Amer. Ceramic Soc. 44(10). 513-522, October 1966.

9. Bernard J. Alley, Hiram W. H. Dykes: Packing of Multicomponent Mixtures of Ammonium Perchlorate and Aluminum Powders, Report RK-TR-66-6, U.S. Army Missile Command, Redstone Arsenal, Alabama, March 1966.

10. Scott, Q. D., Nature, Vol. 188, December 10, 1960, pp. 908-9.

11. Visscher, W. M. and Bolsterli, M., Nature, Vol. 239, October 27, 1972, pp. 504-7.

APPENDIX

Fluidized Powder Density

The mass of the fluidized powders is composed of the mass of the solids plus the mass of gas in the mixture. Density of the two phase mixture is determined as follows:

$$\text{Density} = \frac{\text{Mass (Solids + Gas)}}{\text{Volume}}$$

$$\rho_{s+g} = \frac{W_s + W_g}{\text{Volume}} \qquad (3)$$

Fluidization gas occupies the interstitial volume between the powder particles under static conditions. During expulsion additional gas may enter the bed due to pressure drop associated with acceleration, friction and leakage effects.

If additional gas enters the bed during flow conditions then the volume fraction of gas increases. Modification of equation (3) gives:

$$\rho_{s+g} = \frac{W_s + W_{gt}}{1 + (1-x)\, \dot{W}_{gi}/\dot{W}_{gs}} \qquad (4)$$

For example during fire Test No. 100, considering AP:

$$W_{gs} = \frac{PV}{RT}(1-x)$$

$$= \frac{604(\ 1)(1-.57) \times 144}{55.2\ (532)}$$

$$W_{gs} = 1.27 \text{ lb/unit volume}$$

From the displacement potentiometer transducer the volumetric flow rate measured during this test was 0.0246 cu ft/sec. The weight flow rate of gas was then:

$$\dot{W}_{gs} = 1.27\ (0.0246) = 0.0312 \text{ lb/sec}$$

In addition, the fluidization gas weight flow rate measured during test ($\dot{W}_{gi}$) was 0.0117 lb/sec, and the specific weight (W_{gi}) was 0.0117/(0.0246) = 0.475 lb/unit volume. The total weight of gas in the control volume (W_{gt}) increases:

$$W_{gt} = W_{gs} + W_{gi}$$

$$= 1.27 + 0.475$$

$$W_{gt} = 1.745 \text{ lb}$$

Substituting in equation (4) using the bed calibration data (see Table XII)

$$\rho_{s+g} = \frac{(0.0405)(1728) + (1.745)}{1 + (1-0.57)(0.0117/0.0312)}$$

(AP) $$\rho_{s+g} = \frac{70 + 1.745}{1 + 0.16} = 61.8 \text{ lb/cu ft}$$

From the above calculation it can be seen that the gas volume fraction increased from 0.47 to 0.59.

At injection conditions the gas expands isothermally from 600 psia to 300 psia and therefore the gas volume fraction increases from 0.59 to 1.18

and $$\rho_{s+g} = \frac{70 + 1.745}{.57 + 1.18} = 41 \text{ lb/cu ft}$$

Similarly for Al with methane fluidization gas it can be shown for test number 100 that

(Al) ρ_{s+g} = 94.7 lb/cu ft at tank conditions

ρ_{s+g} = 73.1 lb/cu ft at injection conditions.

Comparison calculations which were made for Test No. 121 follow:

Conditions	Density ρ_{s+g}, lb/cu ft	
	Test 121	Test 100
AP		
at Tank Pressure	71.8	61.8
at Injection Pressure	59.7	41
Al		
at Tank Pressure	96.2	94.7
at Injection Pressure	80.8	73.1

It can be seen that the resulting density values differ somewhat which is due to variations in test conditions. AP differed in particle size while Al variations were attributed to pressure and fluidization gas. Correspondly, actual injection velocity differed from design values stated in Table III.